MCW 1465

AEC Research and Development Report

CONTRACTOR FOR U.S. ATOMIC ENERGY COMMISSION

PROCESS DEVELOPMENT QUARTERLY PROGRESS REPORT

August 1, 1961

Mallinckrodt®

WELDON SPRING PLANT

MALLINCKRODT CHEMICAL WORKS

URANIUM DIVISION

Contract No. W-14-108-Eng-8

DISCLAIMER

LEGAL NOTICE

Printed in USA. Price $1.25 Available from the Office of Technical Services, Department of Commerce, Washington 25, D.C.

MCW-1465

August 1, 1961

UC-47, Technology - Feed Materials
(TID-4500, 16th Ed.)

PROCESS DEVELOPMENT QUARTERLY PROGRESS REPORT

April - June 1961

MALLINCKRODT CHEMICAL WORKS
URANIUM DIVISION
Weldon Spring, Missouri

Contractor for the
U. S. Atomic Energy Commission
(Contract No. W-14-108-Eng-8)

The work reported in this document was done under the general supervision of:

J. H. Yeager
Technical Director

J. A. Fellows and A. E. Ruehle
Assistant Technical Directors

R. F. Hartmann, Manager
Metallurgical Development

A. E. Ruehle, Acting Manager
Chemical Technology

W. A. Ziegler, Manager
Analytical

E. I. Miller, Director
Manufacturing

The publication of this document was directed by

J. A. Nelson

DISTRIBUTION

	No. of Copies
Internal	25
External	
In accordance with TID-4500, 16th Edition	499
American Radiator and Standard Sanitary Corporation	1
Bureau of Mines, Reno, Mr. T. R. Graham	1
Division of Production, Washington, Mr. W. Devine	1
Dow Chemical Company, Rocky Flats, Dr. L. A. Matheson	1
du Pont Company, Aiken	
Dr. M. H. Wahl	1
Mr. T. C. Evans	1
Dr. R. T. Huntoon	1
Fernald Area Office, Mr. C. L. Karl	1
General Electric Company, Richland	
Mr. A. G. Blasewitz	1
Dr. S. H. Bush	1
Mr. S. M. Gill	2
Mr. L. H. McEwen	1
Mr. J. E. Minor	1
Mr. J. T. Stringer	1
Mr. E. A. Weakley	1
Mr. F. W. Woodfield	1
Mr. L. L. Zahn	1
National Lead Company of Ohio	
Dr. M. A. DeSesa	1
Mr. C. E. Polson	1
Dr. F. L. Cuthbert	1
Nelco Metals, Inc., c/o Oak Ridge Operations Office	1
Oak Ridge Operations Office	1
Mr. B. M. Robinson	1
Dr. R. E. Wedemeyer	1
Mr. E. B. Kiser, Jr.	1
	550

CONTENTS

INFRARED ABSORPTION ANALYSIS OF URANIUM TRIOXIDE

by

H. E. Peña

SUMMARY

The infrared absorption spectra of uranium trioxide produced by Mallinckrodt Chemical Works, Eldorado Mining & Refining Limited, and National Lead Company of Ohio are presented. In addition to the identification of uranium-oxygen groups and nitrate functional groups, it was found that a relationship exists between the observed band intensity at 11.5 microns and the rate of hydrofluorination of the reduction product of uranium trioxide. The influence of increasing concentrations of ammonium hydroxide and ammonium sulfate on the observed band intensity at 11.5 microns is also illustrated by comparing the recorded spectra.

INTRODUCTION

Chemical methods for analyzing uranium trioxide products do not show which of the polymorphic types of the compound have been produced. Neither do they show changes in the uranium trioxide that have been interpreted to indicate a more reactive product. Accordingly, the use of infrared spectroscopy for the qualitative and quantitative analysis of uranium trioxide products has been studied.

The vibrational spectrum is directly related to the structure of a solid crystalline compound. This relationship is based on the unit cell of the crystal and not on individual molecules. The symmetry of the arrangement of the molecules within the unit cell is related to the intensity of the absorption bands. However, strong modifications of the spectrum would be produced by the presence of strong intermolecular forces. One may, therefore, expect to find significant differences among the spectra of uranium trioxide, since it exists in polymorphic forms. Just as X-ray studies permit recommendations of a structural classification of types of polymorphic materials, so do infrared absorption studies allow the identification of uranium trioxide modifications. In the case of uranium trioxide, the modifications are associated with changes in structure characterized by thermal effects and by effects due to inorganic additives.

The known polymorphic phases of uranium trioxide consist of five crystalline modifications and one amorphous form. The infrared spectra of the six types of uranium trioxide in the 2.5- to 15.0-micron region have been published by Hoekstra and Siegel.[1] Although uranium trioxide exhibits a number of polymorphic phases, there is no indication of why a particular phase should appear at the temperature that it does. The significant differences between the various uranium trioxide modifications are identified by their infrared spectra

as possible changes in the valence angle of oxygen in the structure. These modifications are necessarily connected with a change in character of the chemical bond from more covalent to more ionic or vice versa. Since in the thermal decomposition of uranyl nitrate hexahydrate several crystalline modifications of uranium trioxide may be produced, it is important to know the relationship between the various phases. Knowledge of the effect of a particular phase of uranium trioxide on the product quality of the material is highly desirable. Quality in the present discussion refers to the hydrofluorination reactivity of the uranium trioxide's reduction product.

EXPERIMENTAL

Preparation of Samples

Application was made of the potassium bromide pressed pellet technique.[2] Pellets produced in a die were rectangular in shape, 25.4 x 5 x 0.55 mm, and had an average weight of 190 ± 6 milligrams. Pellets were prepared with 0.50% uranium trioxide in AR-Grade potassium bromide. Each uranium trioxide sample was ground and mixed with an agate mortar and pestle before pellet preparation. The mixtures of 0.50% uranium trioxide in potassium bromide were ground for 3 minutes in stainless steel vials on a Wig-L-Bug vibrator. Absorbance measurements were made using the standard base-line technique and normalizing to a pellet weight of 200 milligrams. Weighings were made on an Ainsworth micro-balance and a torsion balance.

Absorption Measurements

The infrared spectra were obtained by means of a Beckman IR-4 infrared spectrophotometer equipped with sodium chloride prisms. The instrument was provided with recorder chart gears that enabled the presentation of a compressed recorded spectrum. A linear absorbance attachment permitted the recording of sample data in terms of absorbance. The prisms of the spectrophotometer were calibrated in the 11.0-micron region by referring to the band at 11.028 microns reported by Plyler[3] et al. in the spectrum of polystyrene.

Reactivity Data

Reactivity data received on Eldorado Mining & Refining uranium trioxide samples were reconfirmed by thermogravimetric analysis. Laboratory standard conditions were used for the analysis.

The rate of hydrofluorination was determined by first plotting the percent of uranium dioxide converted to uranium tetrafluoride as a function of time in minutes. The resulting area under the plotted curve was determined by using a compensating polar planimeter. Smaller areas under the plotted curve indicate greater rates of reaction. All areas were determined up to 36 minutes unless the plotted curve crossed the abscissa in less time.

RESULTS AND DISCUSSION

Qualitative Analysis of Uranium Trioxide Produced by Batch Denitration

Variations in the Spectra of Mallinckrodt Production-Grade UO_3

Figure 1 and Fig. 2b show the spectra of samples of Mallinckrodt uranium trioxide that were produced at different times. These spectra indicate variations in production conditions by the variation in intensity of the 11.2-micron band. The 11.2-micron band was graphically extrapolated to emphasize the variation in its concentration from one sample to the next. The 11.2-micron band is ascribed to the presence of ϵ-type UO_3 in admixture with Type-III UO_3. Figure 2a shows the spectrum of Type-III UO_3.

Spectra of Uranium Trioxide Formed as a Cake in the Batch Process

During the thermal denitration of uranyl nitrate by the batch process, a cake material is formed around the agitator shaft and on the walls of the pot. The cake may be separated into three parts: (a) hard yellow material, (b) soft spongy yellow material, and (c) a black material. Figure 3 shows the spectra obtained from the different parts that constitute the cake. The spectrum of Fig. 3a is similar to that of normal uranium trioxide. Figure 3b shows the spectrum of pure Type-III UO_3 (seldom obtained as a unique product in Mallinckrodt batch-denitrated uranium trioxide), and Fig. 3c shows the spectrum of U_3O_8 with a small amount of uranium trioxide.

Comparison of the Spectra of UO_3 Produced by MCW, NLO, and Port Hope

It is of interest to record and compare the differences found in the spectra of uranium trioxide produced by Mallinckrodt Chemical Works, National Lead Company of Ohio, and Eldorado Mining & Refining Limited, at Port Hope, Ontario, Canada. The spectra are shown in Fig. 4. They differ not only in the content of ϵ-type UO_3 (indicated by the band at 11.2 microns), but also in the intensity of the Type-III UO_3 band at 11.5 microns. The residual nitrate content can be compared at 7.2 microns.

Changes in Structure Characterized by Thermal Effect in NLO UO_3

The infrared absorption spectra of uranium trioxide produced by the National Lead Company of Ohio changed from predominantly Type-III UO_3 to predominantly ϵ-type UO_3 in October, 1960. Because the NLO uranium trioxide that is currently produced is predominantly ϵ-type UO_3, it was used in a study of the effects of heating the product to 500°C for the same length of time both in air and in an inert atmosphere. The infrared spectra of the samples were recorded before and after heating the samples.

Figure 4 (c and d) shows the spectra of uranium trioxide produced by NLO in the months of September, 1960, and October, 1960. The spectra

of uranium trioxide samples produced after October, 1960, are similar to the October sample but show a decrease in the residual nitrate content, as indicated by the 7.2-micron band, which is due to the asymmetric vibration of the nitrate ion. Figure 5 shows the spectraof NLO uranium trioxide produced in October, 1960, after heating to 525°C both in air and in argon. These spectra show that heating NLO uranium trioxide, which is predominantly ϵ-type UO_3, will effect the transition to the Type-III phase. The intensity of the band at 11.5 microns of the resulting Type-III UO_3 appears to be affected by whether the heating process took place in air or in an inert atmosphere.

Spectra of the Sieve Fractions of Port Hope and MCW UO_3

The spectra of U.S. Standard Sieve fractions of Eldorado Mining & Refining uranium trioxide produced by batch denitration are identical to the spectrum shown in Fig. 4b. The spectra of all the sieve fractions may be identified as Type-III UO_3 with very small amounts of ϵ-type UO_3 (indicated by a shoulder on the 11.5-micron band). Also, the residual nitrate content (7.2 microns) was found to be exceptionally low in all the sieve fractions. Of even greater significance is the intensity of the absorption bands. None of the spectra of the sieve fractions showed the 11.5-micron band to have an absorbance of less than 0.800 unit, while some sieve fractions had an absorbance of 1.000 unit. All the spectra indicated, by the sharpness of the 12.4- and 13.7-microns bands, a more crystalline type of material.

Figure 6 shows the spectra of U.S. Standard Sieve fractions of Mallinckrodt uranium trioxide produced by batch denitration at Weldon Spring. These spectra show considerable variation. The large particles (-40 to +70) have spectra that may be identified as Type-III UO_3 containing very small amounts of other uranium trioxide modifications. The spectra of the rest of the sieve fractions show that although Type-III UO_3 is present, there is a variation in the content of other polymorphic forms of uranium trioxide, their band intensities, and the residual nitrate content. Figure 6b shows the spectrum of the uranium trioxide present in 30% of the sample analyzed.

Quantitative Analysis of Uranium Trioxide Produced by Batch Denitration

The Relationship Between the Observed Intensity of a Band at 11.5 Microns of Type-III UO_3 and the Rate of Hydrofluorination

Evidence that is currently available (Table I) on uranium trioxide samples from Eldorado Mining & Refining Limited shows that the intensity of the 11.5-micron band of Type-III UO_3 markedly increases with an increase in the rate of hydrofluorination. The samples analyzed represented lot composites and were also representative of high and low reactivity by Port Hope standards.

Such a large change as shown in the intensity of the 11.5-micron band for Port Hope uranium trioxide has never been observed in

Mallinckrodt production-grade uranium trioxide. Therefore, it has not been possible to compare Mallinckrodt uranium trioxide reactivity with uranium trioxide band intensity in the same manner.

Table I

A Comparison of the Infrared Absorption of Uranium Trioxide at 11.5 Microns to the Rate of Hydrofluorination of Its Reduction Product - Lot Composite Samples of Uranium Trioxide from Eldorado Mining & Refining Limited

Lot Composite	Absorbance[a] at 11.5 μ	Area Under Hydrofluorination Rate Curve[b] cm^2
53-57	0.720	56.2
58-66	0.767	49.8
173-177	1.078	21.1
178-182	1.198	19.4

[a]Normalized to pellet weight of 200 mg.

[b]Smaller areas indicate greater rates of reaction.

Changes in the Intensity of the Band at 11.5 Microns of Type-III UO_3 Due to Inorganic Additives

By comparison of absorption intensities of the infrared spectra of Type-III UO_3 one can readily ascertain that there exist limits to the admixture of foreign substances. The samples analyzed are intended to show the changes that take place in the spectra of uranium trioxide upon the addition of inorganic compounds.

1. Addition of Ammonium Hydroxide

The spectra of experimental batch-denitrated uranium trioxide to which 10,000 ppm and 30,000 ppm of ammonia, on a uranium basis, were added as ammonium hydroxide during denitration are shown in Fig. 7. The addition of ammonium hydroxide at a level of 10,000 ppm ammonia (Fig. 7a) produced a Type-III UO_3 that is free of any other type of uranium trioxide and can be compared to the uranium trioxide produced at Port Hope. The intensity of the 11.5-micron band is nearly identical to that of the most reactive (conversion to UF_4) Port Hope product that has been analyzed in this laboratory. The residual nitrate content is about 19% of the amount normally found in Mallinckrodt production-grade uranium trioxide.

Figure 7b shows the spectrum of uranium trioxide produced after the addition of 30,000 ppm of ammonia as ammonium hydroxide. The spectrum indicates ε-type UO_3 and Type-III UO_3 and is essentially that of production-grade uranium trioxide even to the intensity of the 11.5-micron band (Type-III UO_3).

Table II compares the intensity of the 11.5-micron band and the rate of hydrofluorination as determined for each experimental sample. The two samples described above show a relationship similar to that of Port Hope uranium trioxide.

Table II

A Comparison of the Infrared Absorption of Uranium Trioxide at 11.5 Microns to the Rate of Hydrofluorination of Its Reduction Product - Uranium Trioxide Produced Experimentally

Figure No.	Additive, Expressed as PPM NH_3		Absorbance[a] at 11.5 μ	Area Under Hydrofluorination Rate Curve[b] cm^2
7a	NH_4OH	10,000	1.030	21.9
7b		30,000	0.715	56.1
8a	$(NH_4)_2SO_4$	980	0.982	--
8b		1,590	0.788	31.9
8c		3,750	0.773	24.3
8d		4,120	0.587	35.6
8e		10,200	0.385	35.7

[a]Normalized to a pellet weight of 200 mg.

[b]Smaller areas indicate greater rates of reaction.

2. Addition of Ammonium Sulfate

The spectra of uranium trioxide produced from uranyl nitrate hexahydrate containing 980 ppm, 1,590 ppm, 3,750 ppm, 4,120 ppm, and 10,200 ppm ammonia, respectively, on a uranium basis, added as ammonium sulfate are shown in Fig. 8. It is this series of samples that clearly shows that there exist limits on the addition of inorganic compounds. As the ammonium sulfate concentration was increased, the intensity of the 11.5-micron band of the uranium trioxide product decreased. Figure 8e shows that denitration was not complete in the sample with highest sulfate concentration, and Fig. 8f shows the spectrum of the uranium trioxide after the removal of residual uranyl nitrate (20%) by extraction with absolute methanol. The major constituent is ε-type UO_3.

The rates of hydrofluorination for these experimental samples as compared to the observed band intensity at 11.5 microns (Table II), do not show the relationship that is prominent with the lot composite samples from Port Hope and the experimental samples containing ammonium hydroxide as an additive.

The addition of foreign constituents in the crystal lattice will influence such characteristics as surface formation and particle size. Both of these properties will definitely influence the results obtained by thermogravimetric analyses. Another variable in the thermogravimetric analysis of uranium trioxide is introduced in the analytical procedure itself. Before a sample of uranium trioxide is reduced with hydrogen, the sample is heated in an inert atmosphere to a temperature of 500°C for approximately thirty minutes. Any amount of uranyl nitrate present in the uranium trioxide sample is converted to uranium trioxide. Therefore, the resulting sample of uranium trioxide would necessarily indicate a rate in accord with the type of uranium trioxide that was produced on preheating the original sample.

Interpretation of the infrared spectrum of the sample represented by Fig. 8e shows that denitration for this sample was incomplete. Even so, the rate of hydrofluorination for this particular sample is equivalent to that of the sample whose spectrum, shown in Fig. 8d, is more like the spectrum of normally produced uranium trioxide.

CONCLUSION

The discussion in this report has shown that interpretation of phase behavior of uranium trioxide can be made primarily on the basis of infrared absorption analysis. Functional groups can be recognized in the uranium trioxide spectra and attributed to various degrees of denitration. Furthermore, data obtained from lot composite samples indicate that limits on the reaction rates may be predicted from information obtained by comparing absorption intensities at 11.5 microns. Comparison of absorption intensities in the spectra of uranium trioxide having variations in concentration of the inorganic additives studied shows that there is a limiting value to the admixtures.

Infrared analysis has also shown that batch-denitrated uranium trioxide produced at controlled temperature, and with ammonium hydroxide as an additive, produces a Type-III UO_3 crystal with a very strong absorption at 11.5 microns. The spectrum of uranium trioxide produced in this manner is identical to that of the most productive Port Hope uranium trioxide analyzed in this laboratory.

ACKNOWLEDGMENT

The author is very grateful to L. G. Weber for providing the Port Hope samples and making available the data on these samples, and to J. D. Vie, who provided the thermogravimetric analysis data.

References

[1]Hoekstra, H. R., and Siegel, S., "The Uranium-Oxygen System: U_3O_8 to UO_3," Proc. Intern. Conf. Peaceful Uses Atomic Energy, Geneva, 1955, 28, 231-4 (1958).

[2]Stimson, M. M., and O'Donnell, M. J., J. Am. Chem. Soc. 74, 1805-8 (1952).

[3]Plyler, E. K., Danti, D., Blaine, L. R., and Tidwell, E. D., "Vibration-Rotation Structure in Absorption Bands for the Calibration of Spectrophotometers from 2 to 16 Microns," N.B.S. Monograph 16 (1960).

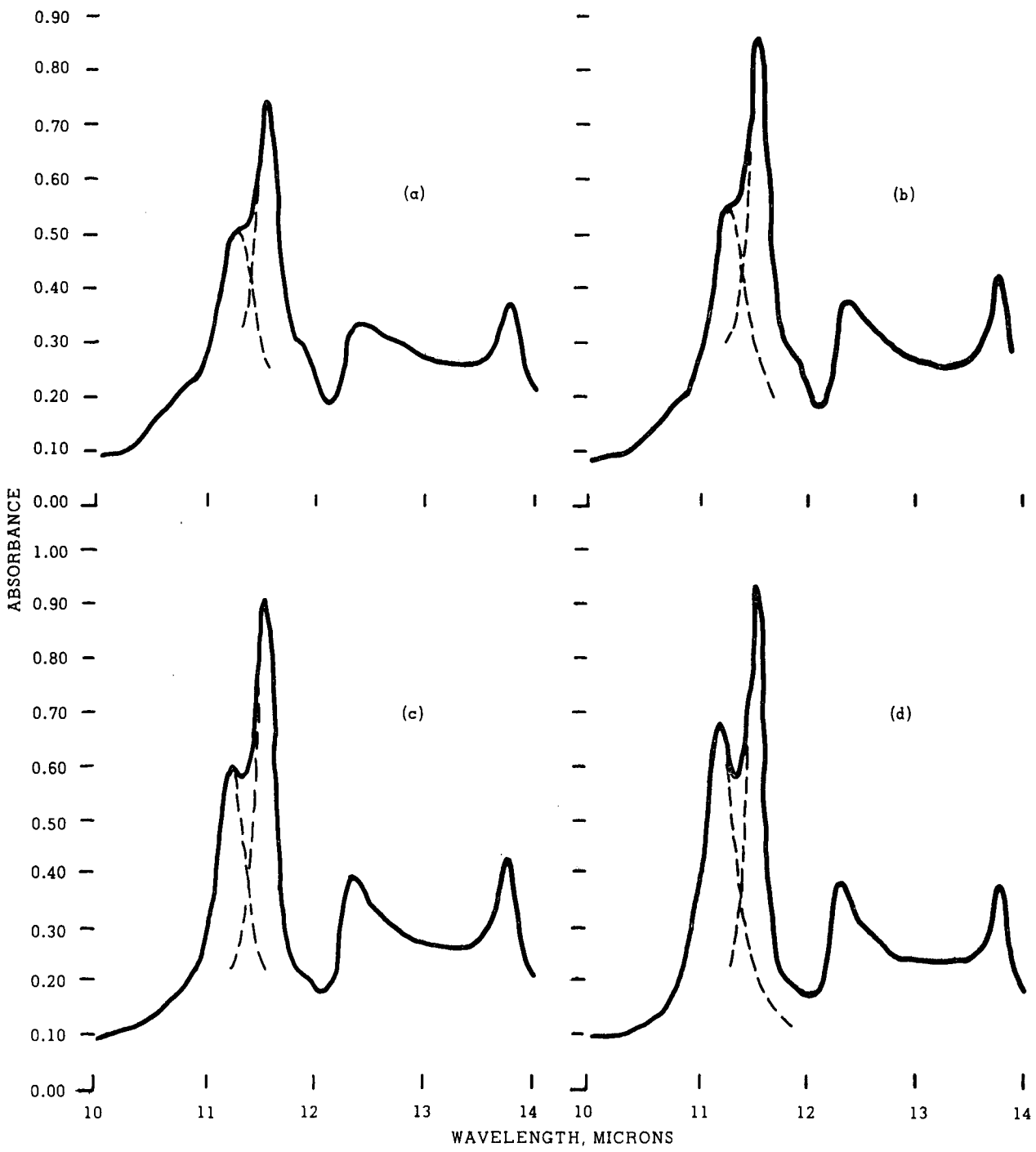

Fig. 1. Comparisons of the Infrared Absorption Spectra of Mallinckrodt Production-Grade, Batch-Denitrated UO_3 Products: (a) Normal; and (b), (c), and (d) Not Normal. KBr pellet technique.

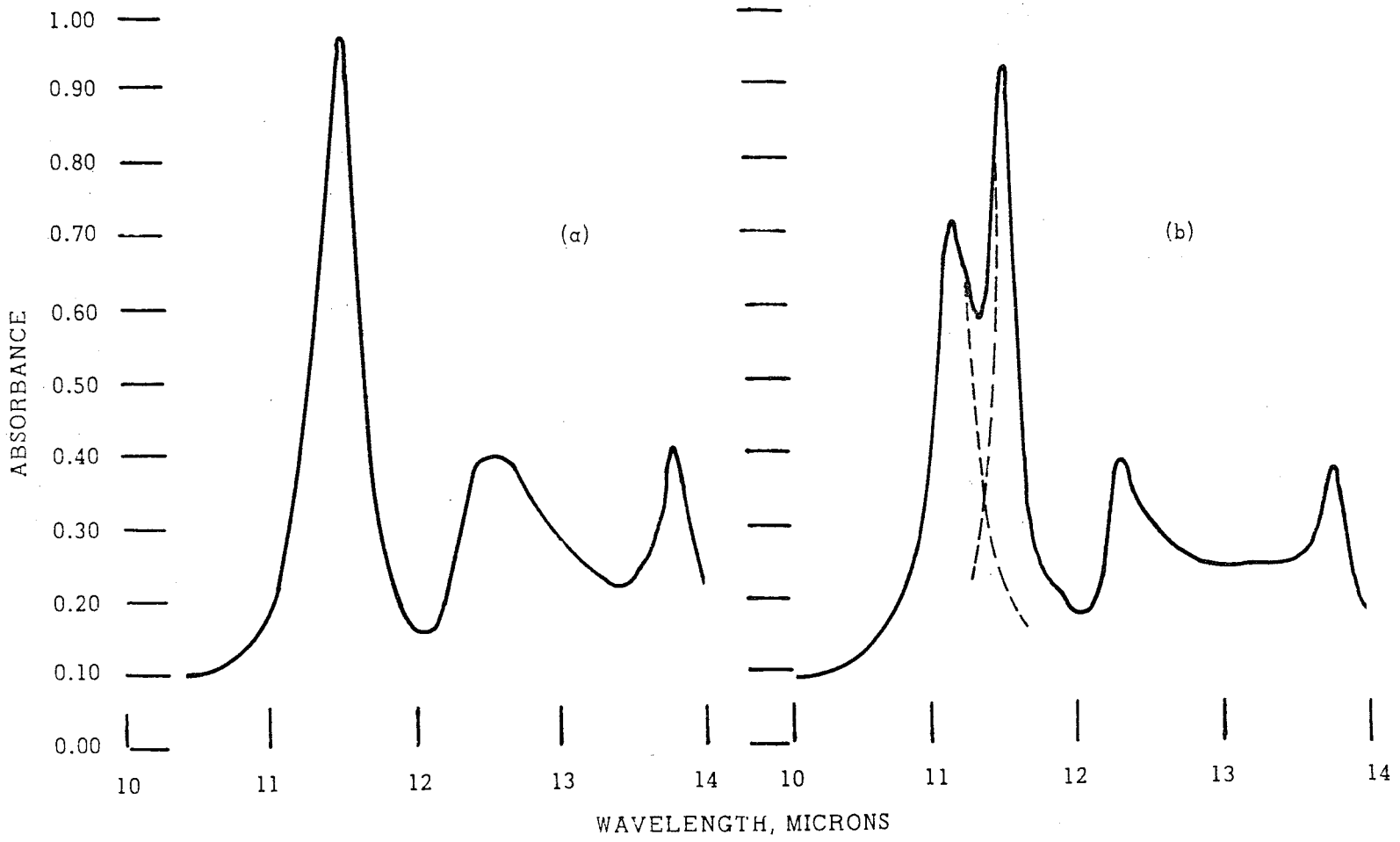

Fig. 2. Comparison of the Infrared Absorption Spectra of (α) Type-III UO_3 and (b) a Mixture of Type-III and ε-Type UO_3. Mallinckrodt batch denitration products. KBr pellet technique.

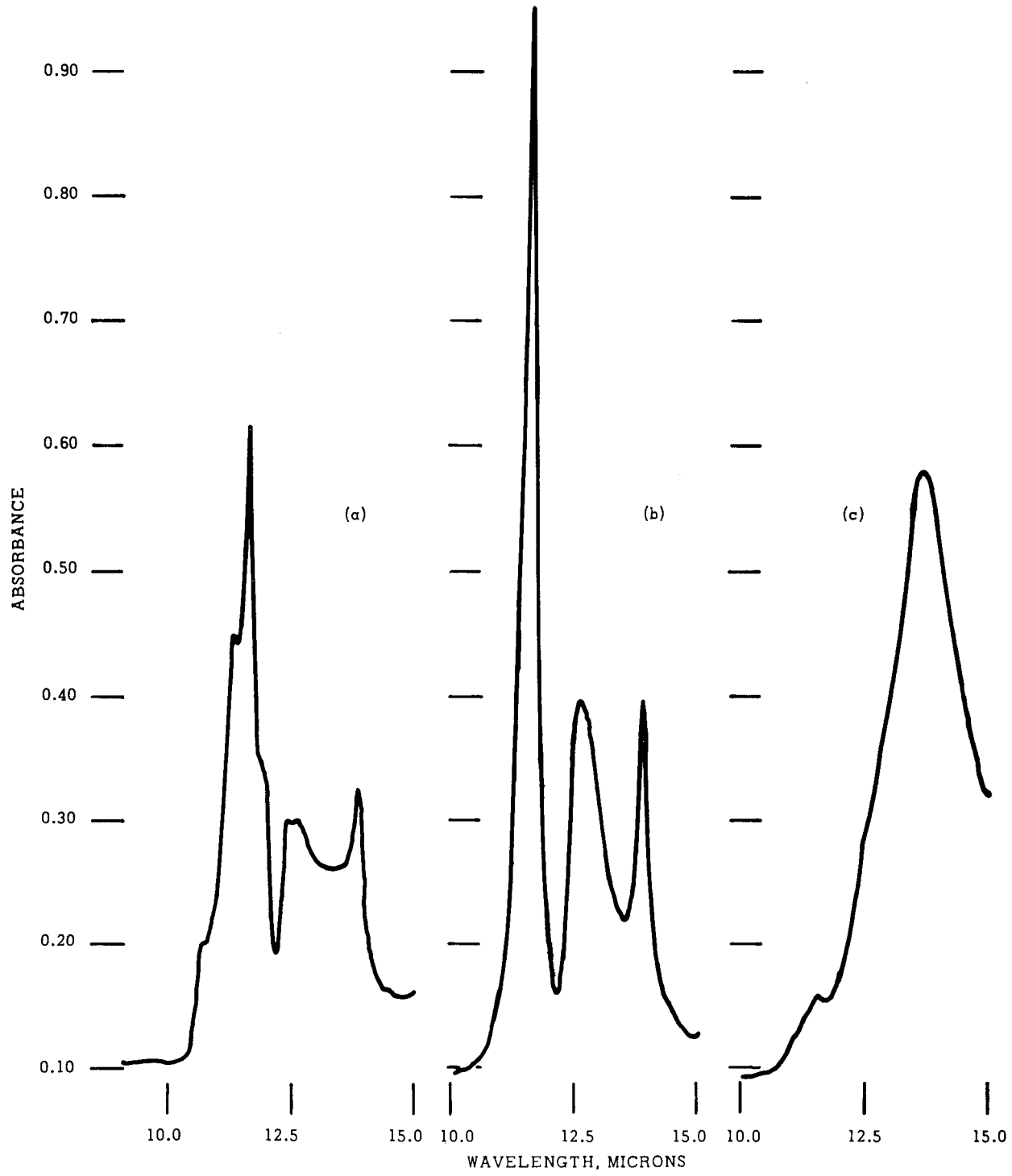

Fig. 3. Infrared Absorption Spectra of Cake Produced by Batch Denitration of UNH. KBr pellet technique.

(a) Hard yellow material,

(b) Soft sponge yellow material,

(c) Black material.

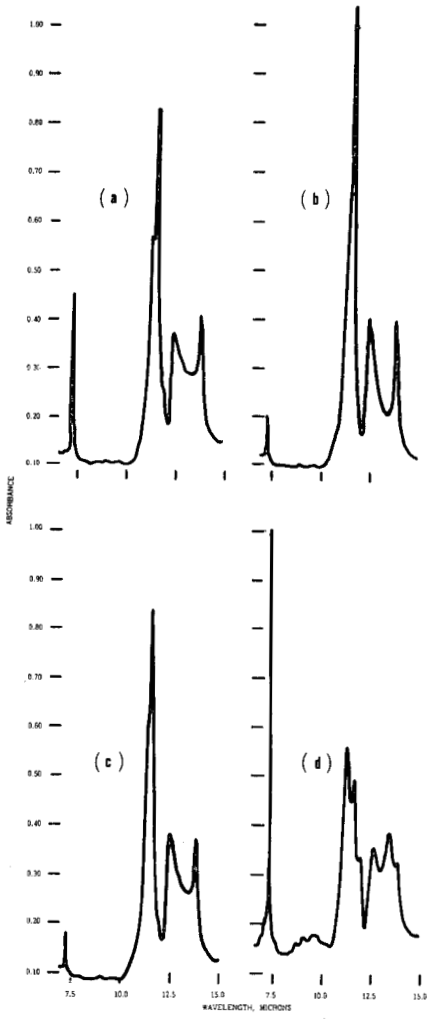

Fig. 4. Infrared Absorption Spectrum of Batch-Denitrated, Production-Grade UO_3. KBr pellet technique.
(a) Mallinckrodt; (b) Eldorado Mining and Refining Limited;
(c) NLO, September 1960; (d) NLO, October 1960.

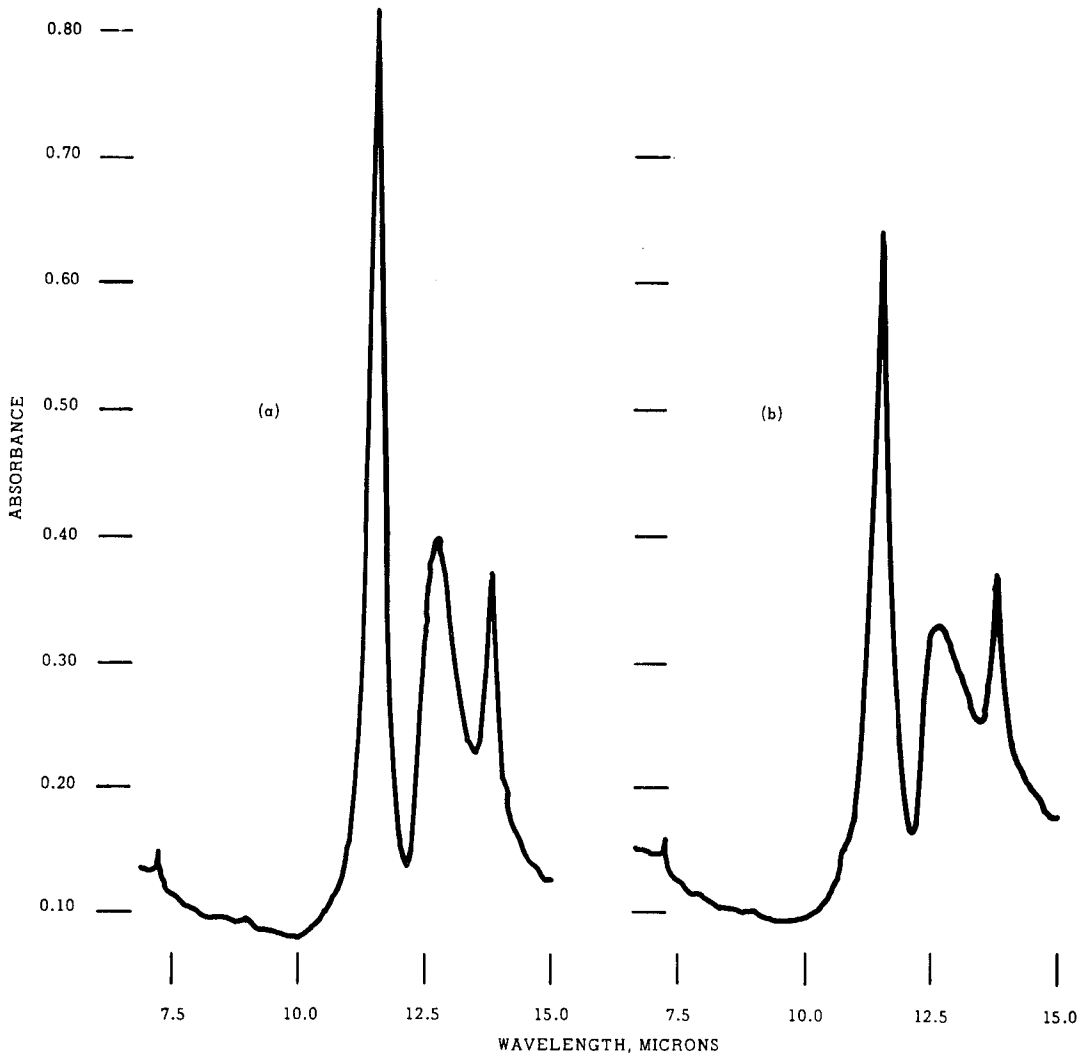

Fig. 5. Comparison of the Infrared Absorption Spectra of NLO Batch-Denitrated UO_3 Produced in October 1960: (a) Heated in Argon to 525°C and (b) Heated in Air to 525°C. KBr pellet technique.

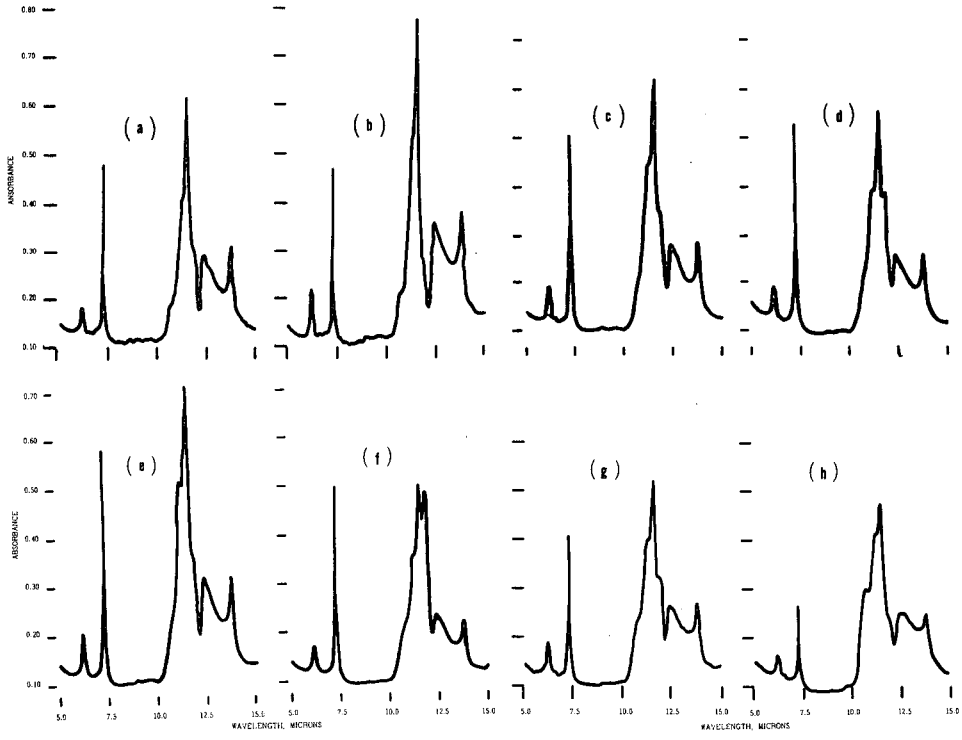

Fig. 6. Comparison of the Infrared Absorption Spectra of U.S. Standard Sieve Fractions of Mallinckrodt Batch-Denitrated UO_3. KBr pellet technique.

(a) -40 +50 Sieve Fraction,
(b) -50 +70 Sieve Fraction,
(c) -70 +100 Sieve Fraction,
(d) -100 +140 Sieve Fraction,
(e) -140 +200 Sieve Fraction,
(f) -200 +230 Sieve Fraction,
(g) -230 +325 Sieve Fraction,
(h) -325 Sieve Fraction.

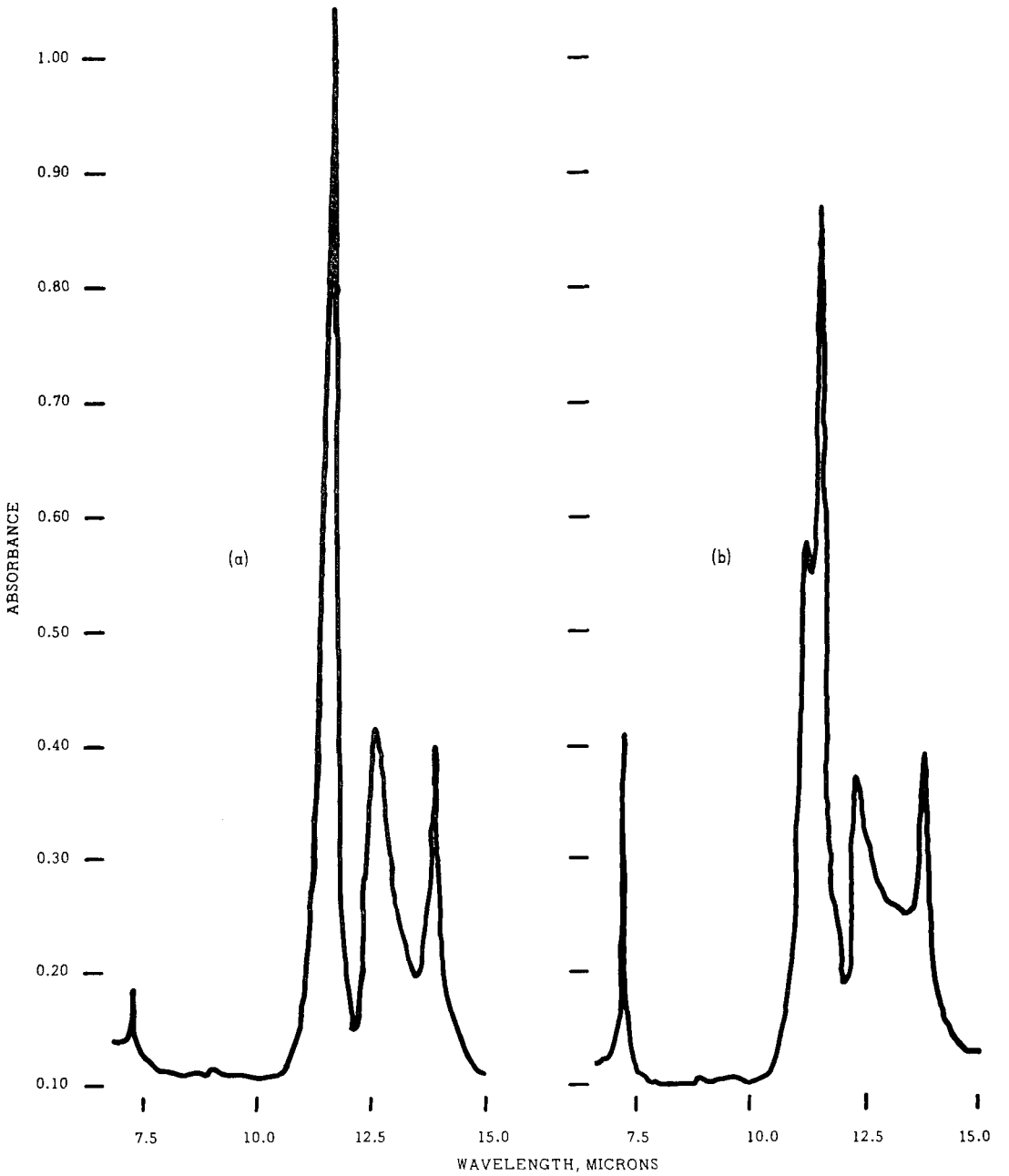

Fig. 7. Infrared Absorption Spectra of UO_3 Produced by Batch Denitration of UNH Containing Ammonium Hydroxide Additions of: (Expressed as PPM NH_3 on a U Basis) (a) 10,000 PPM and (b) 30,000 PPM. Grab samples. KBr pellet technique.

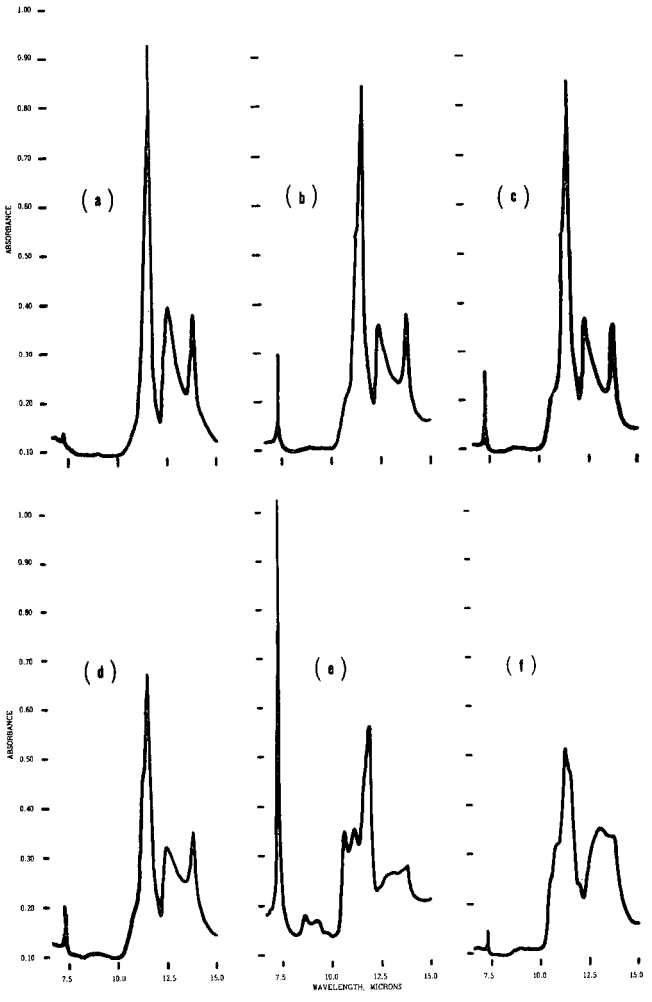

Fig. 8. Infrared Absorption Spectra of UO_3 Produced by Batch Denitration of UNH Containing Ammonium Sulfate Additions of: (Expressed as PPM NH_3 on a U Basis) (a) 980 PPM, (b) 1590 PPM, (c) 3750 PPM, (d) 4120 PPM, (e) 10,200 PPM, and (f) the same as (e) but with the UO_3 Product Extracted to Remove Residual Uranyl Nitrate. Grab samples. KBr pellet technique.

URANIUM RECOVERY FROM SCRAP URANIUM TETRAFLUORIDE BY WET REVERSION WITH SODIUM HYDROXIDE

by

E. P. Grattan*
W. T. Trask

A wet reversion process for the recovery of miscellaneous scrap residues from the Weldon Spring Green Salt Plant has been developed and is being operated in the Chemical Pilot Plant. These residues - normally referred to as C-31 material - consist mainly of impure UF_4 and are currently being reverted at the rate of approximately 35 tons per month. The C-31 material is digested in a hot sodium hydroxide solution to revert the UF_4 to an acid-soluble uranium oxide. The product from this digestion is water-washed by decantation until the fluoride content is below 1.0 percent on a uranium basis and is then digested in hot nitric acid. Hydrated alumina is added to complex any remaining fluoride. The resulting uranyl nitrate solution is returned to the Refinery process stream.

The only difficulties encountered to date have been of a purely mechanical nature. The product from the C-31 reversion process is entirely compatible with the Refinery process. Corrosion problems to date have been minor.

Experimental details and results of the process development will appear in Topical Report MCW-1466.

*Present address, Hercules Powder Company, Wilmington, Delaware.

PARTICLE SIZE DETERMINATION BY THE SEDIMENTATION RECORDING-BALANCE METHOD

(Calculation of a Theoretical Distribution Curve
for a System of Single-Size Particles)

by

W. C. Stoecker

SUMMARY

Further study has been made of the sedimentation recording-balance method for determining particle size distribution in the sub-sieve range.[1] A method has been developed for calculating the weight change of the plummet for an idealized system of single-size particles based on a plummet having the shape of a double cone. By means of this calculation, one inherent error of the method has been evaluated (for the idealized system) and found to be of minor importance.

INTRODUCTION

A new method of particle size analysis based on liquid sedimentation was described in a previous report.[1] It is precise, comparatively rapid, and in good agreement with other methods of analysis for magnesium fluoride liner and other materials tested. Of several inherent errors, the most important is the weight change resulting from the adherence of some particles to the plummet. This was discussed in detail, and a technique was described that was found to reduce the error to an acceptably low value.

The error next in importance was believed to be the effect of using a plummet of finite size, rather than an ideal plummet whose length would be negligible compared with its depth below the surface of the liquid. It was suggested in the earlier report that a mathematical analysis of the effect should be attempted. Such a study has now been made for a system of single-size particles, and the results are presented in this report.

An exact mathematical analysis for the teardrop-shaped plummet actually used in the experiments would be very difficult. However, a simplification may be made by assuming the shape of the plummet to be that of two cones placed end-to-end with bases together. The error is probably somewhat greater for the double cone than for the teardrop shape, since the centroid of volume is further from the base. A double-conical plummet could have been used in the experiments with equal effectiveness but is somewhat more difficult to make.

CALCULATION OF WEIGHT CHANGE OF PLUMMET AND RESULTING PARTICLE SIZE DISTRIBUTION CURVE - GENERAL CASE

Determine the exact change in weight of the plummet resulting from the settling of a suspension of single-size particles. Determine also for such a system,

the distortion of the particle size distribution curve resulting from the use of a plummet that does not have negligible size. Assume that the plummet has a double-conical shape and that particles of a single size are settling according to Stokes' law in a suspension that is uniform at the start of the test. See Fig. 1.

Let

h = depth of suspension interface below surface

h_o = depth of top of plummet

h_c = depth of center of plummet

D_1 = diameter of spherical particles

D = apparent diameter of particles calculated from Stokes' law

η = viscosity of suspension liquid

ρ_1 = density of particles

ρ_2 = density of suspension liquid

ρ_3 = density of initial uniform suspension

t = time

g = acceleration of gravity

w = apparent change in weight of the part of the plummet that is above the suspension interface

W = total change in weight of plummet (top half)

v = volume of plummet above the suspension interface

V = volume of plummet (top half)

k_1 = ratio of cone height $(h_c - h_o)$ to radius

The buoyant force on the plummet (top half) in the suspension is $\rho_3 V$. The total change in weight due to the complete settling of particles is therefore

$$W = (\rho_3 - \rho_2) V, \tag{1}$$

and the change in weight that has taken place when the suspension interface is at some point h between "h_o" and h_c" is

$$w = (\rho_3 - \rho_2) v. \tag{2}$$

Also,

$$\frac{dw}{dh} = (\rho_3 - \rho_2) \frac{dv}{dh} , \tag{3}$$

$$v = \frac{1}{3} \pi \left[\frac{h - h_o}{k_1}\right]^2 (h - h_o) = \frac{\pi}{3k_1^2} (h - h_o)^3 , \tag{4}$$

$$w = \frac{\pi}{3k_1^2} (h - h_o)^3 (\rho_3 - \rho_2) , \tag{5}$$

$$\frac{dv}{dh} = \frac{\pi}{k_1^2} (h - h_o)^2 , \tag{6}$$

$$\frac{dw}{dh} = \frac{\pi}{k_1^2} (h - h_o)^2 (\rho_3 - \rho_2) , \tag{7}$$

and

$$\frac{v}{V} = \frac{w}{W} = \frac{(h - h_o)^3}{(h_c - h_o)^3} . \tag{8}$$

The relationship between the height of the interface (h) and the time (t) is given by Stokes' law, as follows:

$$D_1 = \sqrt{\frac{18\ h\ n}{(\rho_1 - \rho_2)\ g\ t}} , \tag{9}$$

$$h = \frac{(\rho_1\ \rho\ \rho_2)\ g\ D_1^2 t}{18\ \eta} , \tag{10}$$

and

$$\frac{dh}{dt} = \frac{(\rho_1 - \rho_2)\ g\ D_1^2}{18\ \eta} . \tag{11}$$

In calculating the results of a determination according to the normal procedure, the plummet depth is assumed to be constant (h_c), and the particle diameter (D) is considered a function of time (t). The relationship between "t" and the calculated "D" is found as follows, again using Stokes' law:

$$t = \frac{18\ h_c\ \eta}{(\rho_1 - \rho_2)\ g\ D^2} = \frac{18\ h_c\ \eta}{(\rho_1 - \rho_2)\ g} D^{-2} . \tag{12}$$

Therefore,

$$\frac{dt}{dD} = \frac{-36\ h_c\ \eta}{(\rho_1 - \rho_2)\ g} D^{-3} . \tag{13}$$

"D" may also be expressed as a function of "h" by eliminating "t" between Equations (9) and (12):

$$\frac{D^2}{D_1^2} = \frac{h_c}{h} . \tag{14}$$

In order to examine the effect of the weight change on a plot of particle size distribution, it is necessary to know the way in which this change occurs with respect to apparent particle diameter. The required derivative, dw/dD, may be determined as follows:

$$\frac{dw}{dD} = \frac{dw}{dh} \cdot \frac{dh}{dt} \cdot \frac{dt}{dD} \quad . \tag{15}$$

Substituting from Equations (7), (11), and (13):

$$\frac{dw}{dD} = \frac{\pi}{k_1^2} (h - h_o)^2 (\rho_3 - \rho_2) \cdot \frac{(\rho_1 - \rho_2)\, g\, D_1^2}{18\, \eta} \cdot \left[\frac{-36\, h_c\, \eta}{(\rho_1 - \rho_2)\, g} D^{-3} \right] ,$$

which reduces to

$$\begin{aligned} \frac{dw}{dD} &= \frac{-2\, \pi\, D_1^2\, h_c\, (\rho_3 - \rho_2)\, (h - h_o)^2}{k_1^2 \qquad D^3} \quad , \\ &= \frac{-2\, \pi\, h_c\, (\rho_3 - \rho_2)\, D_1^2\, (h - h_o)^2}{k_1^2 \qquad D^2 \qquad D} \quad . \end{aligned} \tag{16}$$

Substituting for D_1^2/D^2 using (14)

$$\frac{dw}{dD} = \frac{-2\, \pi\, (\rho_3 - \rho_2)\, h\, (h - h_o)^2}{k_1^2 \qquad D} \quad . \tag{17}$$

An apparent particle size distribution curve may now be plotted for the mono-sized system if all constants of the experiment are known. With the total weight change of the plummet, the weight change corresponding to any value of "h - h_o" may be determined from Equation (8). The corresponding value of "D" may be found from Equation (14). The slope for any values of "D" and "h" is determined from Equation (17), and reasonably close values of slope may be obtained by replacing Equation (17) with the approximation

$$\frac{dw}{dD} = \frac{-2\, \pi\, (\rho_3 - \rho_2)\, h_c\, (h - h_o)^2}{k_1^2 \qquad D_1} \quad . \tag{18}$$

The second part of the distribution curve resulting from the settling of particles by the lower half of the cone will be approximately symmetrical with the first part. The change in volume (v) and apparent weight (w) of the lower half of the cone as a function of the height of the interface (h) is exactly opposite to the change for the upper part. However, the intervals of "D" become slightly less owing to the tendency of particle diameter (D) to become less dependent on time (t) as time increases.

Equation (14) may be used for calculating any value of "D" corresponding to values of "h" for "h" > "h_c" in the same way as for the upper part of the plummet.

APPLICATION OF THE METHOD OF CALCULATION TO A TYPICAL EXAMPLE

Assume that

$$h_o = 36.8 \text{ cm}$$
$$h_c = 40 \text{ cm}$$
$$D_1 = 20 \times 10^{-4} \text{ cm}$$
$$\rho_3 - \rho_2 = 0.0194 \text{ g/cc}$$
$$k_1 = 4$$

From Equation (4) the volume (V) of the plummet (top half) is found to be 2.145 cc; from Equation (5) the total weight change (W) is 0.04161 g using $h - h_o = h_c - h_o = 3.2$ cm. Assuming various other values of $h - h_o$, corresponding values of "w" and "D" are calculated using Equations (8) and (14), respectively. The slope of the curve at each point is calculated from Equation (18) and converted from grams per centimeter to milligrams per micron by dividing by 10.

Since the usual plot of results shows "weight percent above stated size" as the ordinate instead of weight change, "w" may be converted to this basis as follows:

$$\text{Wt. percent above stated size} = \frac{w}{2W} \times 100.$$

The calculations are tabulated in Table I, and plotted as a particle size distribution curve in Fig. 2.

Table I

Calculation of Weight Change for System of Single-Size Particles

h cm	$h - h_o$ cm	$\frac{(h - h_o)^3}{(h_c - h_o)^3}$	w mg	Wt. Percent above Stated Size	D μ	$\frac{dw}{dD}$ mg/μ
36.8	0	0	0	0	20.86	0
37.3	0.5	0.00381	0.159	0.19	20.70	3.8
37.8	1.0	0.0305	1.27	1.53	20.56	15.1
38.3	1.5	0.1031	4.29	5.15	20.44	34.2
38.8	2.0	0.2441	10.16	12.21	20.30	60.8
39.3	2.5	0.477	19.85	23.85	20.18	95.0
39.6	2.8	0.670	27.87	33.49	20.10	119.
39.8	3.0	0.824	34.29	41.20	20.05	137.
40.0	3.2	1.000	41.61	50.00	20.00	156.
40.2	3.4		48.93	58.80	19.95	
40.4	3.6		55.35	66.50	19.90	
40.7	3.9		63.37	76.15	19.82	
41.2	4.4		73.06	87.79	19.70	
41.7	4.9		78.93	94.84	19.58	
42.2	5.4		81.95	98.47	19.47	
42.7	5.9		83.06	99.81	19.36	
43.2	6.4		83.22	100.	19.24	

In Table II, slopes of the curve at several points calculated from Equation (18) are compared with slopes calculated at intervals between corresponding adjacent points. The latter calculation may be considered an "observed" slope.

Table II

Comparison of Calculated and Observed Slopes

$h - h_o$ cm	$\frac{dw}{dD}$ mg/μ Calculated	$\frac{dw}{dD}$ mg/μ Observed	Interval cm
3.1	146	146	3.0 - 3.2
2.9	128	128	2.8 - 3.0
2.65	107	100	2.5 - 2.8
2.25	77	81	2.0 - 2.5

The agreement noted is a partial verification of the derivation of Equation (18).

Reference

[1]Stoecker, W. C., Process Development Quarterly Progress Report, Mallinckrodt Chemical Works, MCW-1464 (May 1, 1961), p. 43-56.

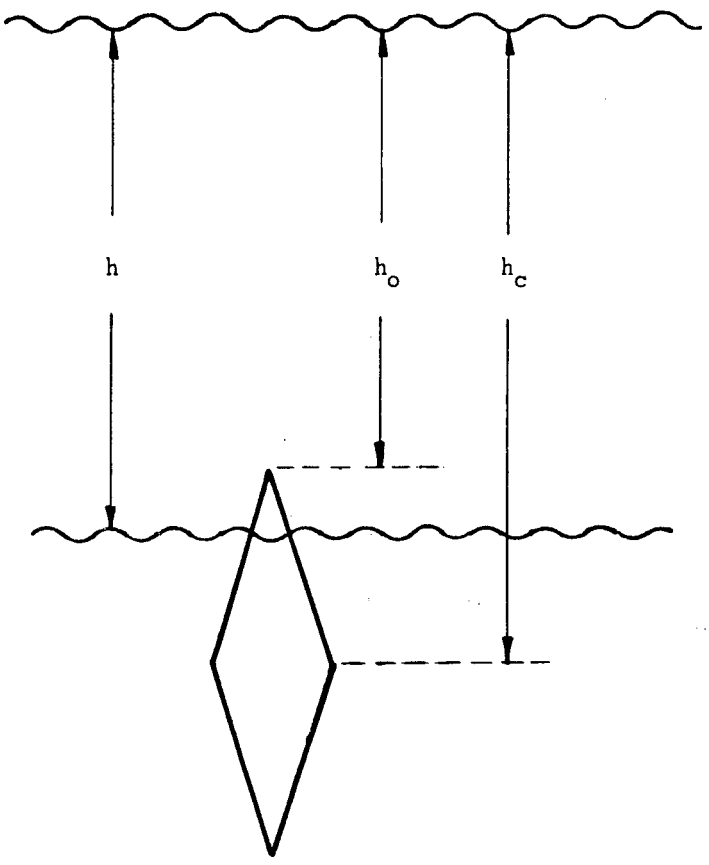

Fig. 1. Location of the Plummet in the Liquid Sedimentation Method for the Determination of Size Distributions in the Sub-sieve Range.

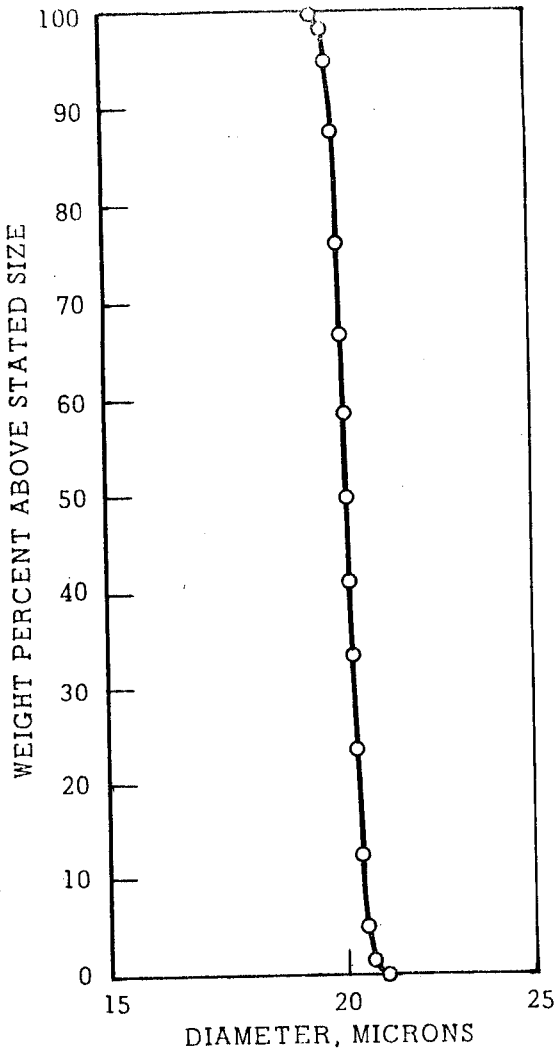

Fig. 2. Calculated Particle Size Distribution Curve for a Suspension of Single-Size Particles (20-Micron Diameter).

THE ALLOYING INFLUENCE OF IRON AND SILICON ON THE GRAIN SIZE OF BETA HEAT-TREATED DINGOT URANIUM

by

J. F. Boland
H. C. Kloepper, Jr.
N. F. Neumann

SUMMARY

When dingot uranium is alloyed with iron and silicon to form a ternary system, a compound is produced that can exist as a fine precipitate in alpha uranium. By varying the heat treatment, this precipitate can be made to grow in size or dissolve in solid solution. Accompanying the change in size and number of undissolved particles is a very pronounced change in the uranium grain size. It is possible that this very fine precipitate acts either as nucleating sites from which grains grow or as particles that block the way for expanding grain boundaries.

INTRODUCTION

The addition of small amounts of iron (100-500 ppm) and silicon (100-300 ppm) to dingot uranium, to form a ternary system, produces a very pronounced change in the beta-treated grain size from that observed in unalloyed dingot uranium. The greater the iron and silicon additions, within the above ranges, the smaller becomes the beta-treated grain size.

Phase diagrams of the individual U-Fe and U-Si systems with the above amounts of alloying elements indicate the presence of U_6Fe and U_3Si, respectively. In a ternary system, however, it was believed that these amounts of alloying elements produce an unknown compound of U-Fe-Si in a uranium matrix. A study was initiated in an attempt to verify the presence of this compound in alloyed dingot uranium core blanks and to learn of its effect on grain structures.

EXPERIMENTAL AND RESULTS

In the preliminary work on this study of the U-Fe-Si system, high-magnification (i.e., 1000X) microscopy identified the presence of a second or "delta" phase in the alpha-uranium matrix of alloyed dingot uranium. This delta phase is present, in the as-rolled metal, as a very finely dispersed precipitate of spherical particles. The relative amount of this precipitate varies with the iron and silicon content.

Soaking in the beta phase (1350°F) for various times, followed by a water quench, eventually dissolved the delta-phase precipitate. For an alloy containing 300 ppm iron and 200 ppm silicon, a period of 4 to 6 hours was necessary to completely dissolve the precipitate. A major portion was observed to disappear after a 15-minute soak.

To investigate the effect of alpha annealing on the delta phase, a sample of hot-worked, alloyed dingot uranium (300 ppm iron - 200 ppm silicon) was annealed for increasing times at 1160°F. The gradual increase of the size of the precipitate with increased time can be seen in Figs. 1-5.

As the temperature of alpha annealing is decreased the delta-phase precipitate shows less tendency to coalesce, as is shown in Fig. 6. Thus, at 1000°F very little particle growth occurs. At higher alpha temperatures, e.g., 1200°F, the coalescence of the delta-phase precipitate with prolonged annealing is accompanied by a large increase in the grain size of the alpha uranium structure (Fig. 7). This effect is in turn passed on to the grain size of the beta heat-treated structure, as is shown in Fig. 8.

Figure 9 shows two samples one of which was alpha annealed at 1020°F and the other at 1190°F, each for a period of 8 hours, and then both were beta heat-treated at 1350°F for 6 minutes. The larger grain size obtained with the sample annealed at the higher alpha temperature corroborates the results presented in Fig. 8. Prolonged periods of beta heat treatment, up to 82 hours, showed no significant change in grain structure from that which occurred with the 6 minute beta treatment (Fig. 8). A double anneal, first at 1200°F, then at 1000°F, for 8 hours each, produced fine grains after a subsequent beta heat treatment (see Fig. 10).

DISCUSSION

In these experiments the form of the delta-phase precipitate was controlled to a certain degree. In doing so, certain correlations were found to exist among the grain size of alpha- and beta-treated structures and the form of the precipitate. The grain size of the beta-treated structure will be small when the delta-phase precipitate is small, finely dispersed and many in number and the grain size of the prior alpha structure is small. Conversely, the grain size of the beta-treated structure is large when the delta-phase particles are large and few in number and the grain size of the prior alpha structure is large.

The grain size of the beta-treated structure is determined during the alpha-to-beta transformation, assuming that a standard quench is performed after the beta treatment. Prolonged soaking in the beta phase, after this transformation has occurred, produces no change in the grain size. One possible explanation for the variation in grain size with annealing temperature is that the delta-phase particles act as nucleating sites for grains that form during the alpha-to-beta transformation. The fewer the number of particles, such as is produced by a long 1200°F anneal, the fewer will be the number of grains in the beta structure and the larger they will be. The opposite would be the case for a finely dispersed precipitate consisting of many small particles. Another possibility is that a few large particles would have much less effect in inhibiting grain growth than would numerous smaller particles.

The terminal solid solubility for the delta phase probably increases with increasing temperature. Thus, when alloyed uranium is annealed at 1200°F, the delta phase will precipitate and coalesce. Rapid cooling of the metal from 1200°F to 1000°F probably results in additional precipitation because of the proposed decrease in solubility. This newly precipitated phase is

probably finely dispersed, as was evidenced by the fine grain size of the beta-treated structure shown in Fig. 10.

ACKNOWLEDGMENT

We wish to thank Messrs. D. L. Parker and M. E. Schafer for their technical assistance in heat treating, sample preparation, and photography.

Fig. 1. "Delta"-Phase Particles in Hot-Worked, Alloyed Dingot Uranium (300 PPM Fe - 200 PPM Si) Alpha Annealed for 6 Hours at 1160°F. Electrolytic etch in ortho phosphoric acid for 7 seconds. Carbon replicate shadowed with uranium, 24,000X.

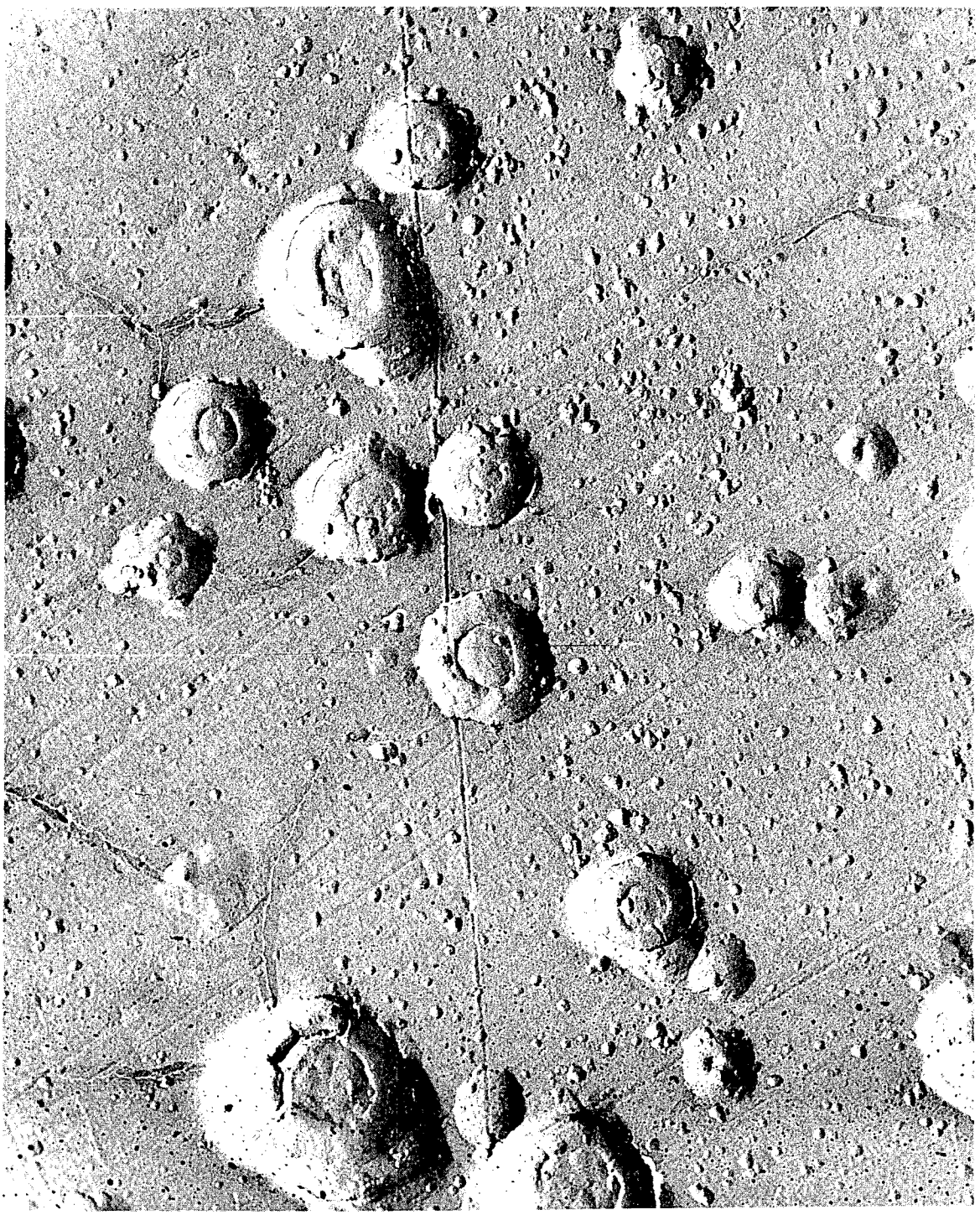

Fig. 2. "Delta"-Phase Particles in Hot-Worked, Alloyed Dingot Uranium (300 PPM Fe - 200 PPM Si) Alpha Annealed for 32 Hours at 1160°F. Electrolytic etch in ortho phosphoric acid for 7 seconds. Carbon replicate shadowed with uranium, 24,000X.

Fig. 3. "Delta"-Phase Particles in Hot-Worked, Alloyed Dingot Uranium (300 PPM Fe - 200 PPM Si) Alpha Annealed for 112 Hours at 1160°F. Electrolytic etch in ortho phosphoric acid for 7 seconds. Carbon replicate shadowed with uranium, 24,000X.

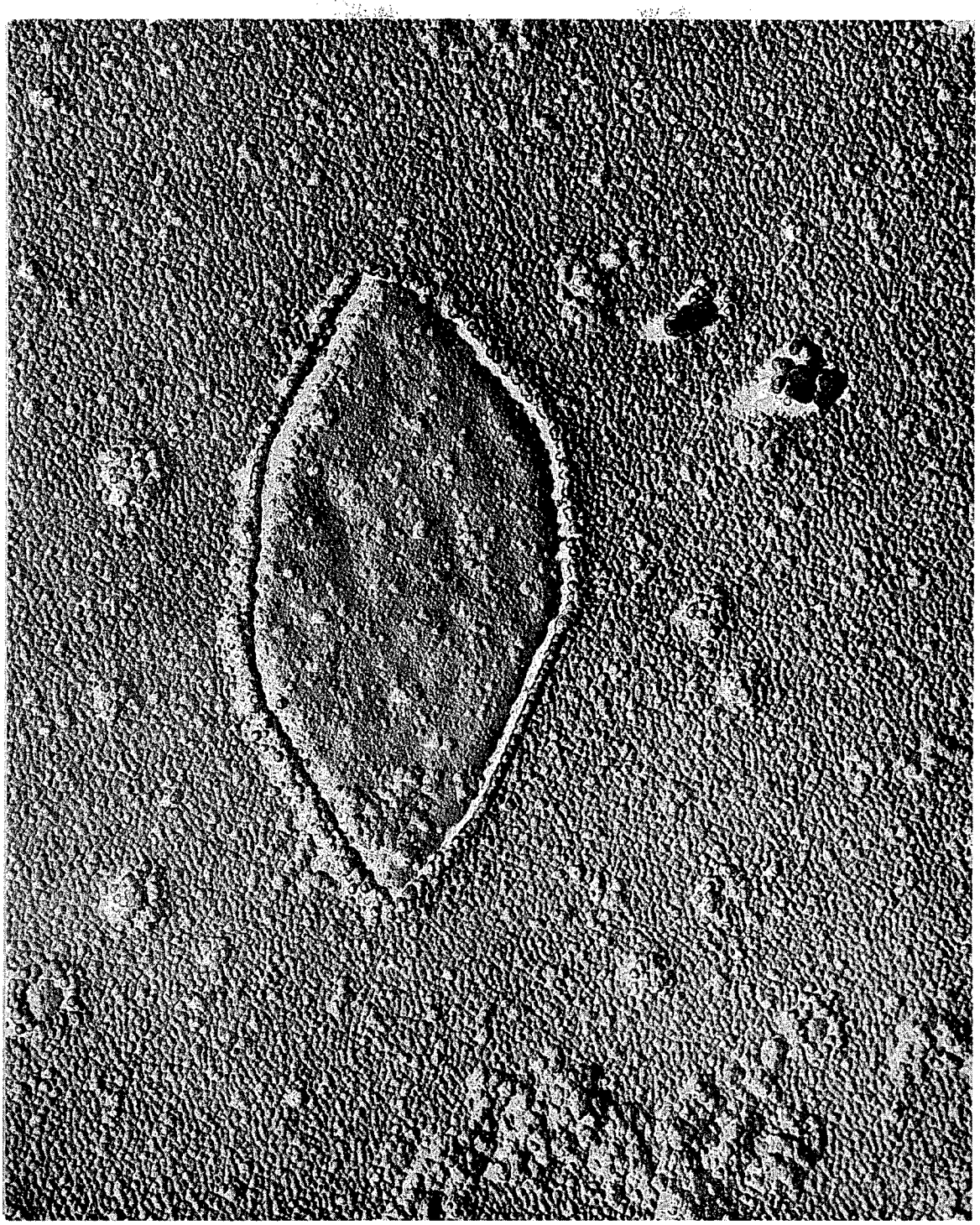

Fig. 4. "Delta"-Phase Particles in Hot-Worked, Alloyed Dingot Uranium (300 PPM Fe - 200 PPM Si) Alpha Annealed for 152 Hours at 1160°F. Electrolytic etch in ortho phosphoric acid for 7 seconds. Carbon replicate shadowed with uranium, 24,000X.

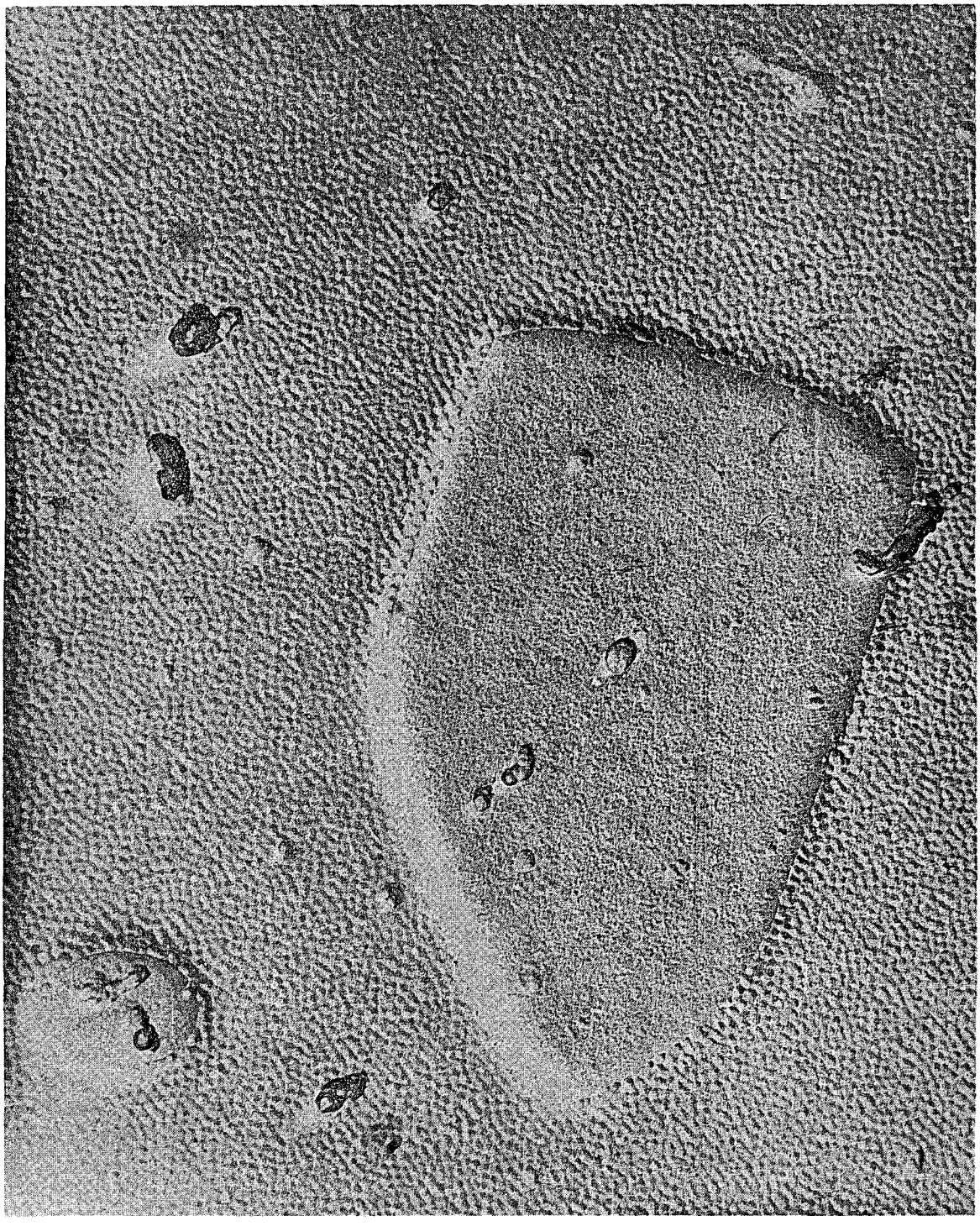

Fig. 5. "Delta"-Phase Particles in Hot-Worked, Alloyed Dingot Uranium (300 PPM Fe - 200 PPM Si) Alpha Annealed for 256 Hours at 1160°F. Electrolytic etch in ortho phosphoric acid for 7 seconds. Carbon replicate shadowed with uranium, 24,000X.

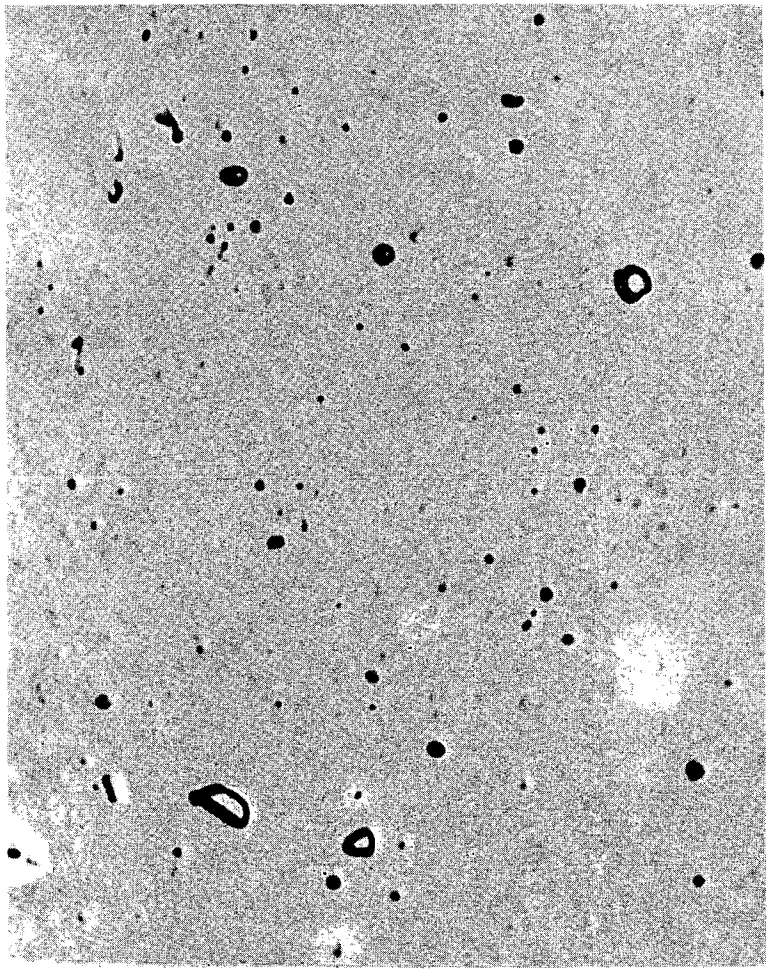

ANNEALED AT 1000°F

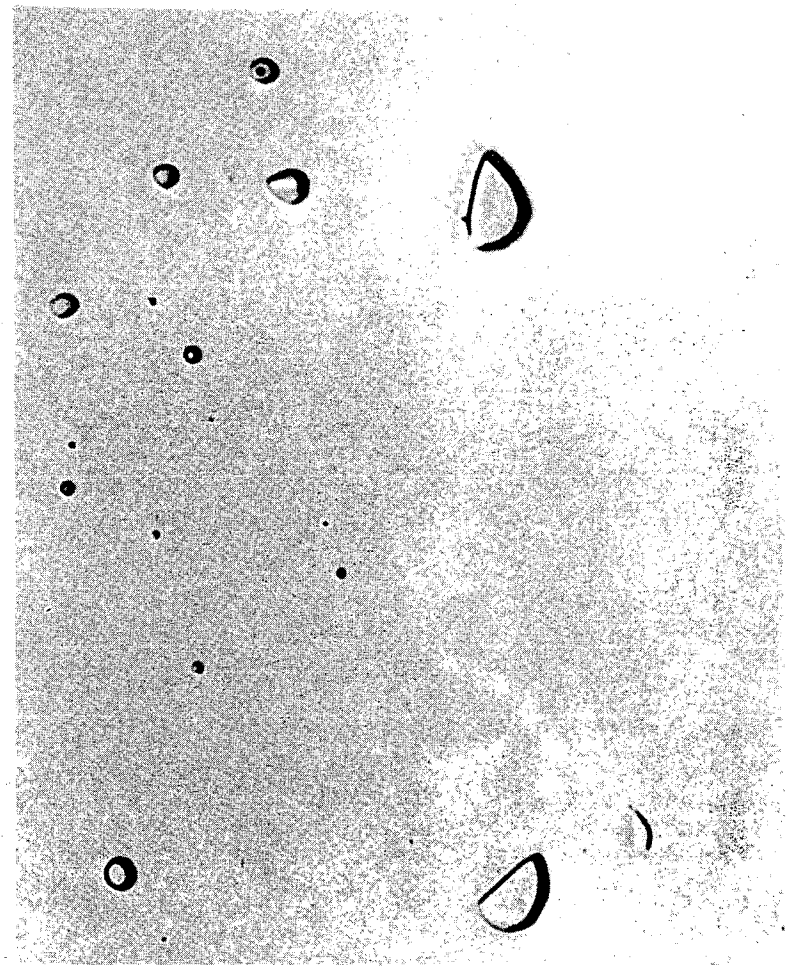

ANNEALED AT 1200°F

Fig. 6. "Delta"-Phase Particles in Alloyed Dingot Uranium (150 PPM Fe - 100 PPM Si) Hot Worked and then Alpha Annealed for 115 Hours. Electrolytic etch in ortho-phosphoric acid for 7 seconds. 2000X.

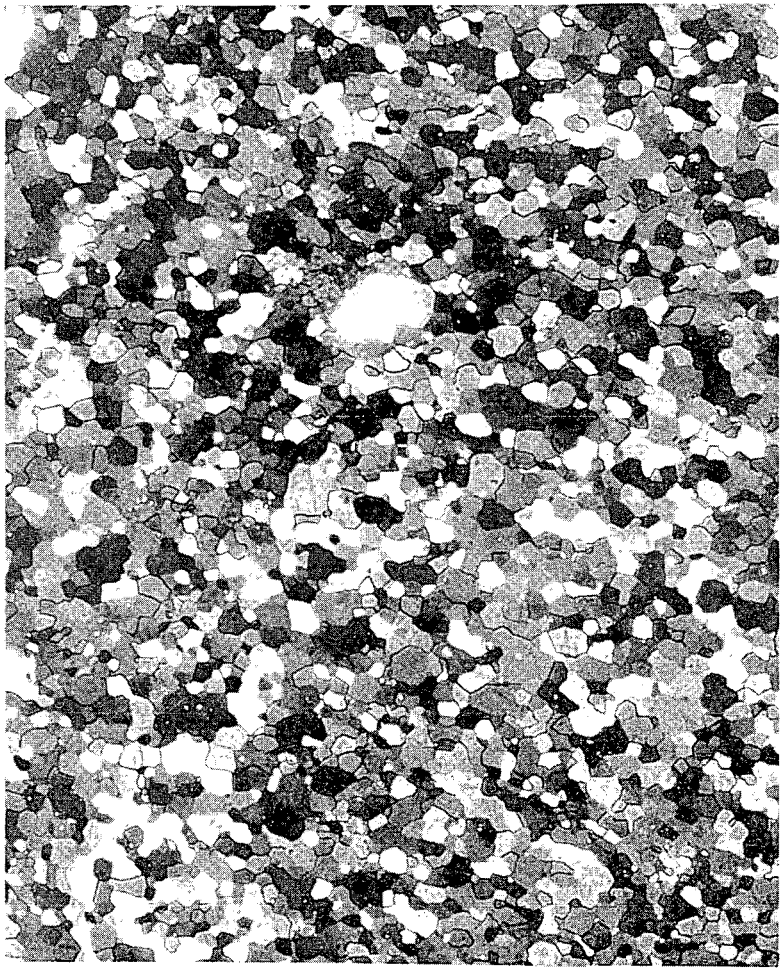

ANNEALED AT 1000°F

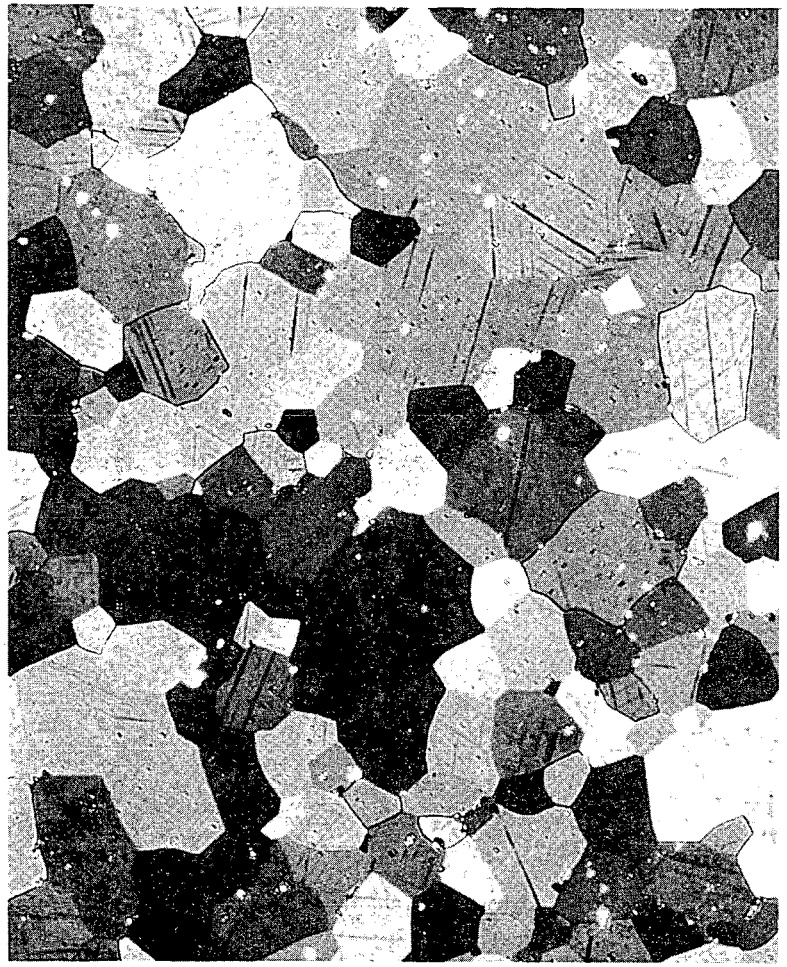

ANNEALED AT 1200°F

Fig. 7. Microstructure of Alloyed Dingot Uranium (150 PPM Fe - 100 PPM Si) Hot Worked and then Alpha Annealed for 115 Hours. Electrolytic etch in chromic-acetic acid for 15 minutes. Polarized light. 200X.

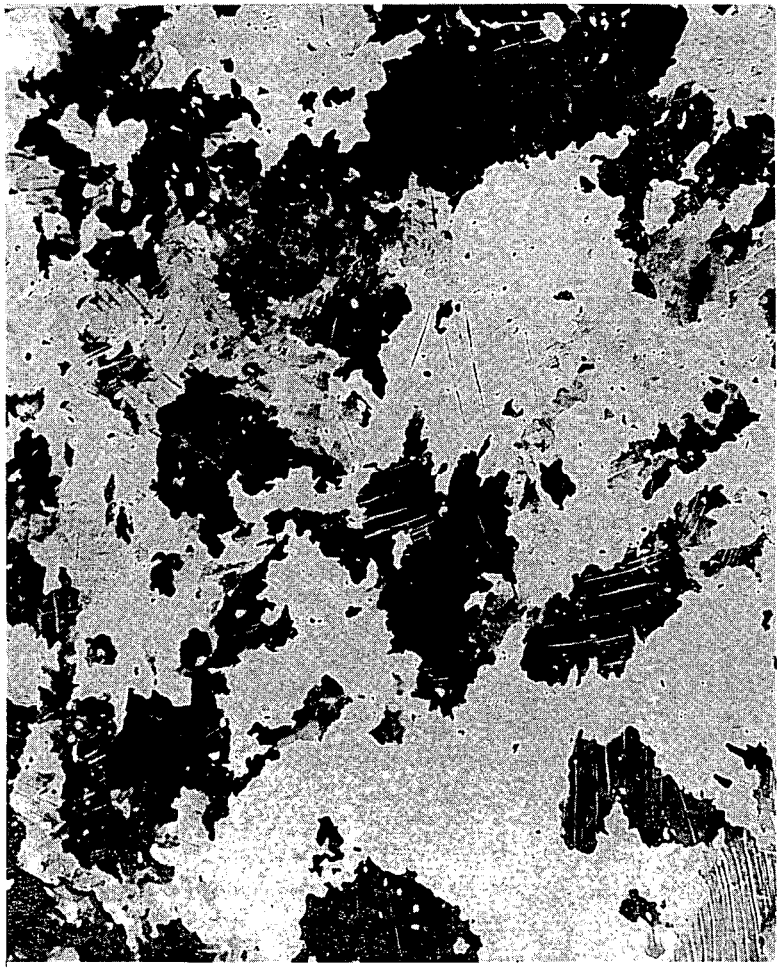

ANNEALED AT 1000°F

ANNEALED AT 1200°F

Fig. 8. Microstructure of Alloyed Dingot Uranium (150 PPM Fe - 100 PPM Si) Hot Worked, then Alpha Annealed for 115 Hours, and then Beta Heat Treated. Electroytic etch in chromic-acetic acid for 15 seconds. Polarized light. 200X.

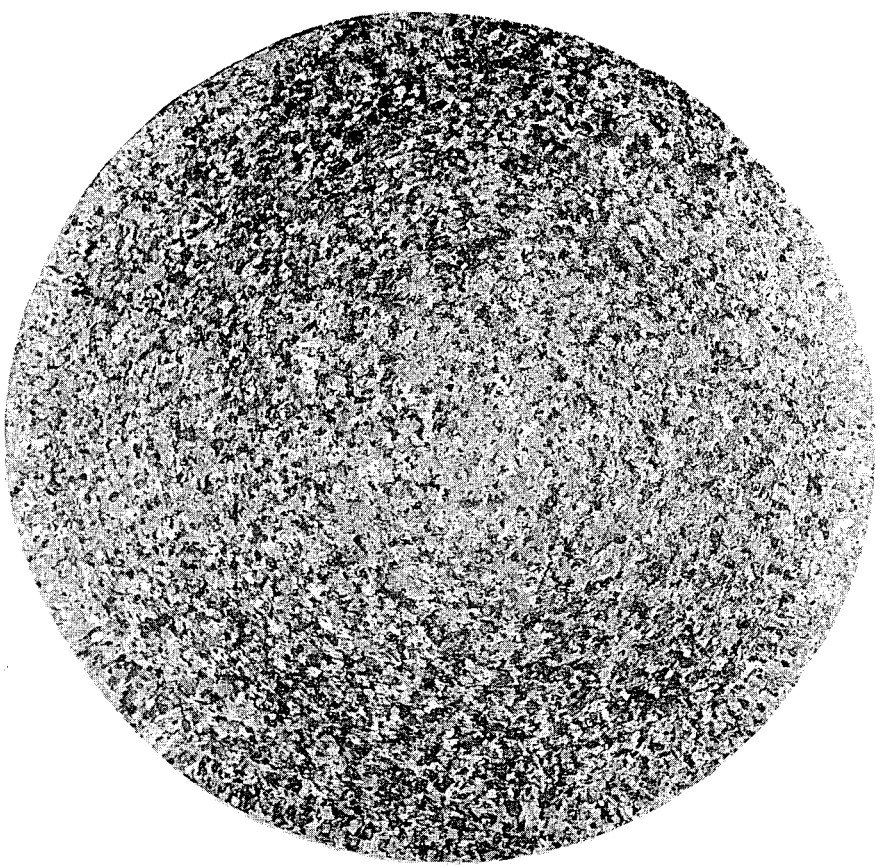

ANNEALED AT 1020°F

ANNEALED AT 1190°F

Fig. 9 Macrostructure of Alloyed Dingot Uranium (150 PPM Fe - 100 PPM Si) Hot Worked, then Alpha Annealed for 8 hours, and then Beta Heat Treated at 1350°F for 6 Minutes and Water Quenched. Etched with hydrochloric acid and then with nitric acid. 3X.

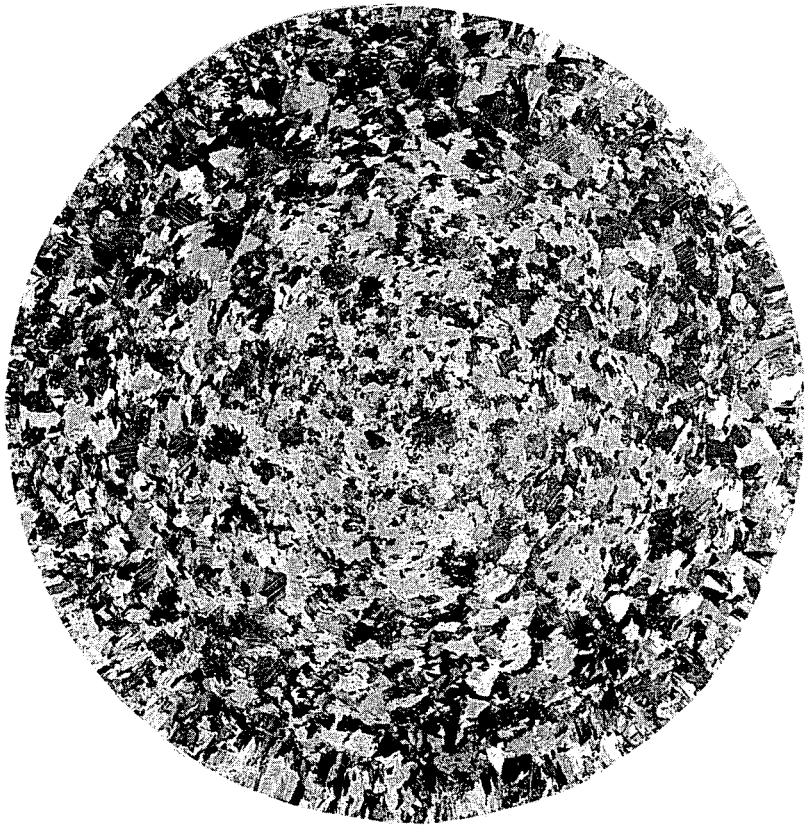

ANNEALED AT 1200°F

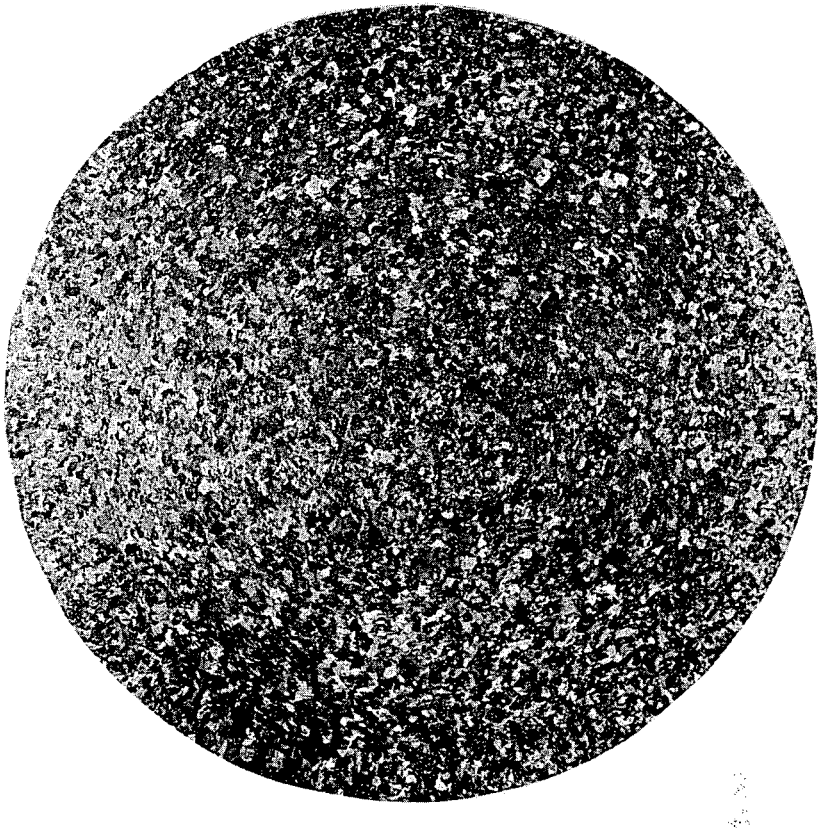

ANNEALED AT 1200°F AND THEN
ANNEALED AT 1000°F

Fig. 10. Macrostructure of Alloyed Dingot Uranium (150 PPM Fe - 100 PPM Si) Hot Worked, then Alpha Annealed First for 8 Hours at 1200°F and then 8 Hours at 1000°F, followed by a Beta Heat Treatment at 1350°F for 15 Minutes and a Water Quench. Etched with hydrochloric acid and then nitric acid. 3X.

THE USE OF A STATHAM PRESSURE TRANSDUCER AS A CONTINUOUS PRESSURE INDICATOR IN VACUUM FUSION ANALYSIS

by

H. F. Waldron

SUMMARY

The standard gage for pressure measurement in an analytical vacuum fusion system is the McLeod gage. To determine a pressure-time relationship with this gage requires several individual pressure measurements over a period of time. In addition, the location of the gage in the system may require an undesirable transfer of the gas to the gage. In most vacuum fusion analyses, it is extremely helpful to have a continuous indication of the pressure in the system. The Statham pressure transducer has been successfully adapted to this use.

INTRODUCTION

The Statham pressure transducer is a strain gage which is sensitive to a difference in pressure across a thin diaphragm that separates two chambers of the gage. This sensitivity is registered in the form of an electrical current which varies linearly according to the magnitude of the pressure differential. When a constant pressure is used as a reference and the gage output is amplified and recorded, a continuous pressure record is obtained. The range of pressure differentials that this recording may register is variable and dependent on the electrical circuitry employed. With the circuitry herein described any one of several ranges may be selected, but 0-750 μ Hg, for a full-scale recorder deflection, is normally used.

In this work, the Statham pressure transducer has been used to continuously monitor the pressure in a vacuum system, with respect to the fore-line pressure, during vacuum fusion analyses. This use provides more complete information, except for the final quantitative measurement, than many laborious transfer and measurement operations with the conventional McLeod gage. The linear response of the gage with respect to pressure permits the very helpful comparison of gas collection rates. Thus, the re-establishment of the blank rate after a sample is degassed may be visually observed by comparison of the recording for the sample to that for a preceding blank. Furthermore, each step during the separation and measurement of the gases may be performed according to the needs of that particular sample rather than according to a pre-determined time schedule, which is always subject to error.

APPARATUS AND EXPERIMENTAL

National Research Corporation's Model 912 vacuum fusion gas analysis apparatus is the basic vacuum unit used for this work. Details of the equipment and its operation have been described by Yeaton.[1] A Statham Pressure Transducer, Model No. PM5TCd $\pm$ 0.15 - 350, supplied by Statham Instruments, Inc., was added to

the system to serve as a direct-reading gage. The gage was sealed into the system near the exhaust port of the circulating diffusion pump to provide maximum pressure information during an analysis. The location of the gage and the gas separation system are shown schematically in Fig. 1.

The Statham gage provides a pressure measurement by comparing the pressure in the system to be measured to the pressure in a reference chamber, as a function of the position of a diaphragm that separates the two chambers. The diaphragm position is monitored by measuring the unbalance of a Wheatstone bridge circuit composed of strain-sensitive wires attached to the diaphragm. This gage is designed for a pressure range of $\pm 10^{-2}$ atmospheres with respect to the reference pressure. However, by appropriate selection of the input voltage, control circuitry, and amplification of the output signal, a small portion of this pressure range can be used to produce a full-scale deflection on a recorder.

The power supply and the control and sensing circuitry for the gage are shown schematically in Fig. 2. The signal output thus obtained is amplified by a Kintel Model 111BF amplifier and recorded by a Leeds and Northrup Speedomax H recorder with a 0- to 10-mv range. When connected in this manner, a 50-fold amplification will produce a full-scale recorder deflection for a pressure change of about 750 μ Hg. For a given amplification, the Helipot, R_1, permits an electrical balance of the gage output so that a recorder indication of zero may be obtained when the pressure differential is considerably greater than that required for a full-scale recorder deflection.

When the Statham gage is used to indicate small pressure ranges, as in this application, the usual method of valving off the reference chamber at a suitable pressure was found to be unsatisfactory. Pressure changes in the reference chamber, due to temperature variations and outgassing, produced intolerable drifts in the recording. The convenient alternate method of using a high vacuum for a reference is undesirable because the thermal insulation results in a higher temperature of operation and shortened life-span of the gage. Therefore, in this system the reference side of the gage has been connected directly to the fore line of the system, as indicated in Fig. 1. With the use of a high-speed fore pump, this method produced a sufficiently stable reference with very short excursions due to increases in the fore pressure when quantities of gas are discharged from the system. The small pressure differential across the gage when the system is under high vacuum may be electrically balanced, as previously described, to provide a recorder indication of zero as a reference point for subsequent pressure measurements.

RESULTS AND DISCUSSION

The use of the continuous pressure-indicating gage has greatly facilitated development work on vacuum methods and it is of considerable aid in routine analyses. Two important features of the gage, for these applications, are the linear response with respect to pressure and the lack of sensitivity with respect to different types of gases. The linearity of response with respect to pressure is verified in Fig. 3. Thus, a direct visual comparison of the slope of the pressure-time recordings for a sample and a blank may be made to determine when the blank rate has been re-established. Furthermore, Fig. 3 could be used to convert recorder deflections directly to the quantity of gas present. For such use, it would be necessary to prepare and use the curve under identical conditions to minimize variations such as temperature. For

example, carbon dioxide released after being frozen at liquid nitrogen temperatures may give a considerably smaller response than expected, even after passing through a diffusion pump. Because of such variables and negligible time savings for final pressure measurements, the gage has been used to provide pressure-change information rather than absolute measurements.

In addition to indicating the total, as removed, gases, a gage located at the exhaust port of the circulation pump (see Fig. 1) permits the monitoring of the pressure when the gases are exposed to the cupric oxide and magnesium perchlorate reactants. This has been used to advantage in the determination of oxygen in uranium by vacuum fusion. In this determination, hydrogen is usually the major constituent evolved and requires considerable time for complete removal from the sample. Collection of the gases directly in the section containing the reactants permits removal of the hydrogen from the gases. About a 5-minute period is required for the initial surge of hydrogen to be removed by the static exposure to the reactants. After this period, the re-establishment of the blank rate may be observed without regard to the lingering hydrogen evolution. A pressure-time recording for an actual sample analysis is shown in Fig. 4. After the re-establishment of the blank rate, the behavior of the system during the various manipulations can be conveniently followed on the recording. The visual evidence of the completeness of each step permits the handling of each sample in an individual manner. Otherwise, a rigid, predetermined schedule, with built-in safety factors for the most adverse conditions, must be followed.

ACKNOWLEDGMENT

The author is indebted to K. A. Cook for the development of the power supply and control circuitry necessary to adapt the Statham gage to this application.

Reference

[1]Yeaton, R. A., Vacuum 2, 115-24(1952).

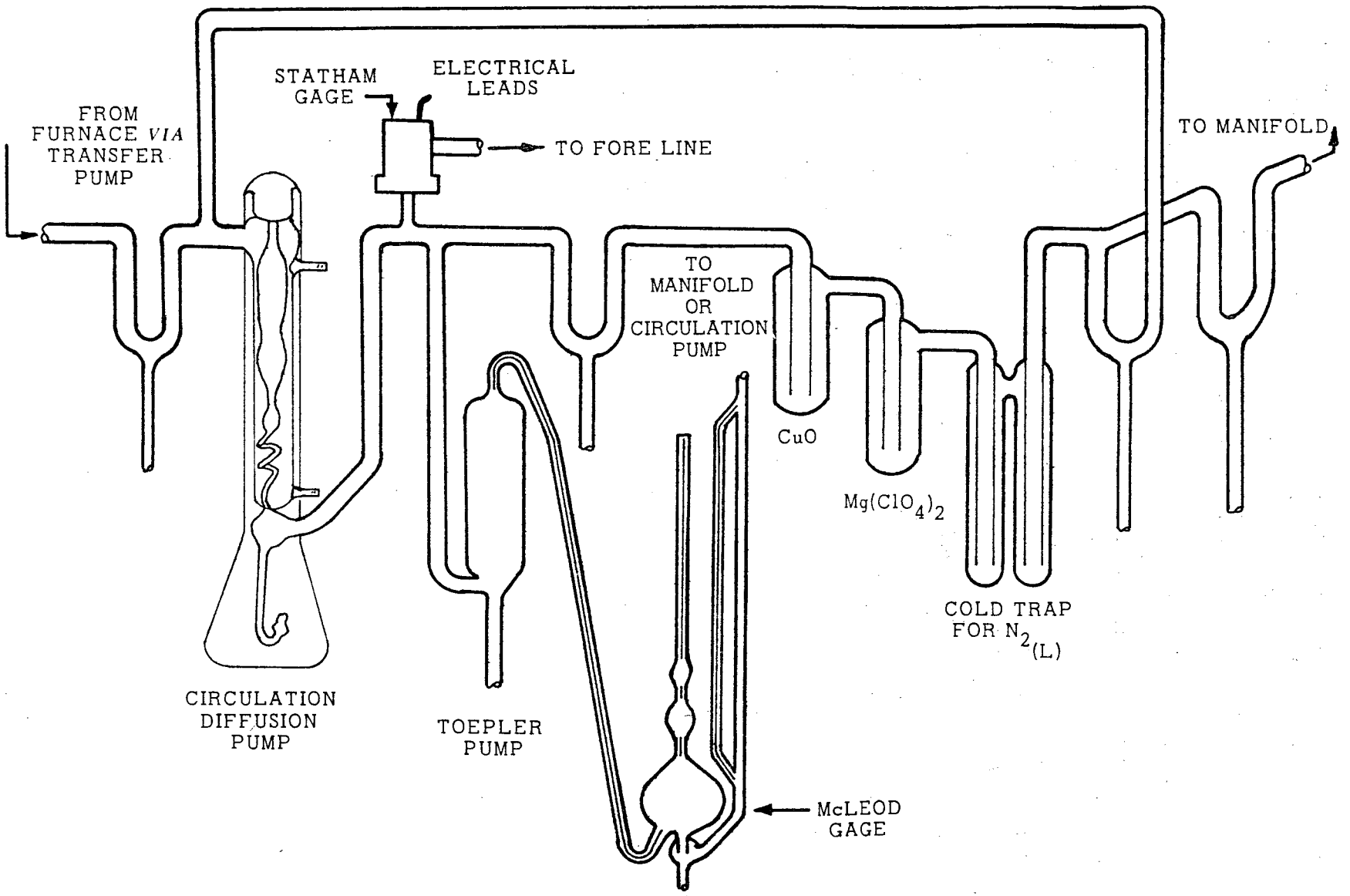

Fig. 1. Schematic Diagram of the Analytical Section of the Vacuum Fusion Apparatus Showing the Location of the Statham Pressure Transducer.

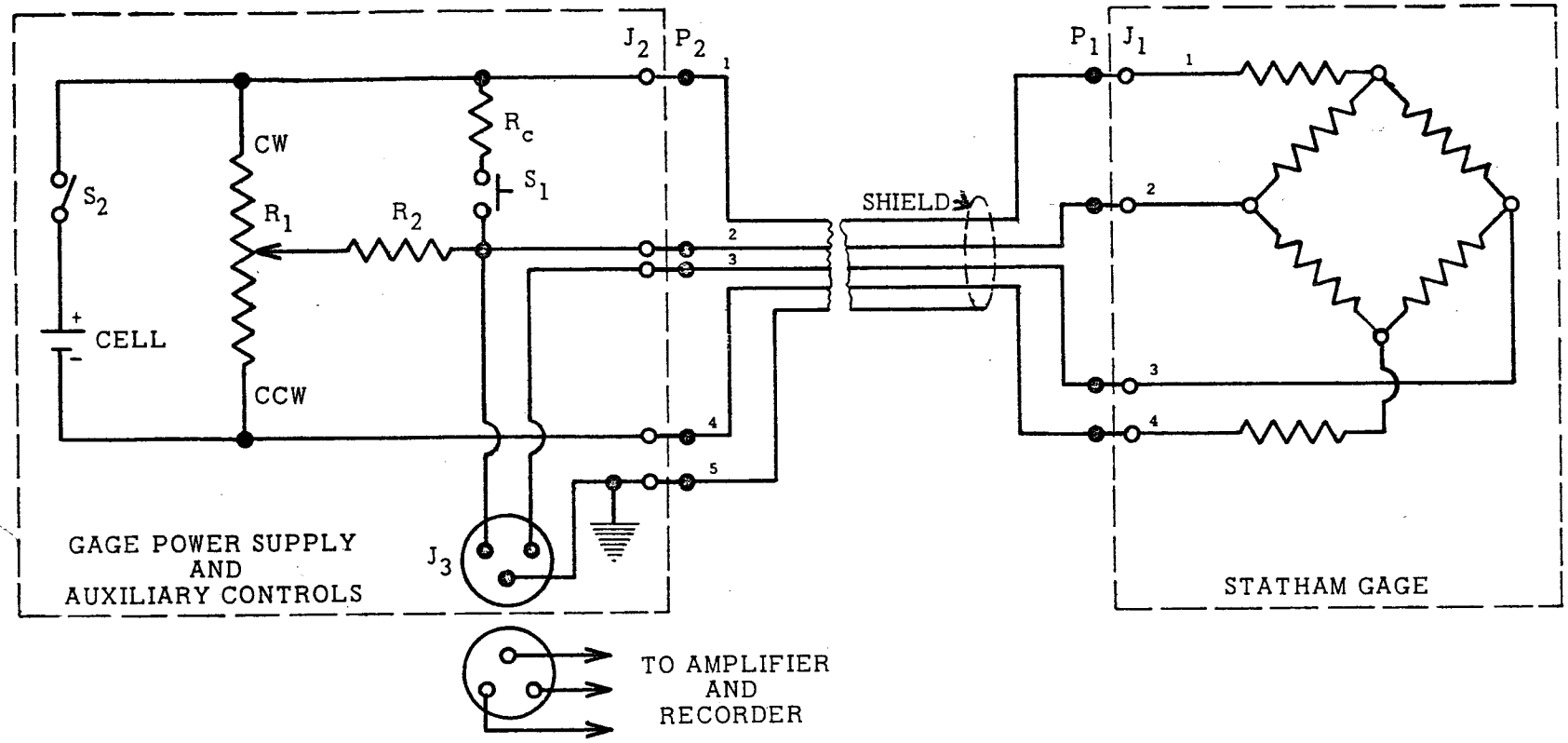

Cell - Mallory Mercury Cell, 1.34 v.
J_1 - Jack on Statham Gage
J_2 - Amphenol 5-Prong Tube Socket
J_3 - 3-Conductor Microphone Jack
P_1 - Plug Supplied with Gage
P_2 - Amphenol 5-Prong Plug
P_3 - 3-Conductor Microphone Plug
R_C - 360-KΩ Precision Resistor
R_1 - 10-Turn Helipot with Duodial, 50 KΩ
R_2 - 47-KΩ Precision Resistor
S_1 - Normally Open, Momentary Switch
S_2 - SPST Toggle Switch

Fig. 2. Circuitry of the Power Supply and Auxiliary Controls Used with the Statham Pressure Transducer.

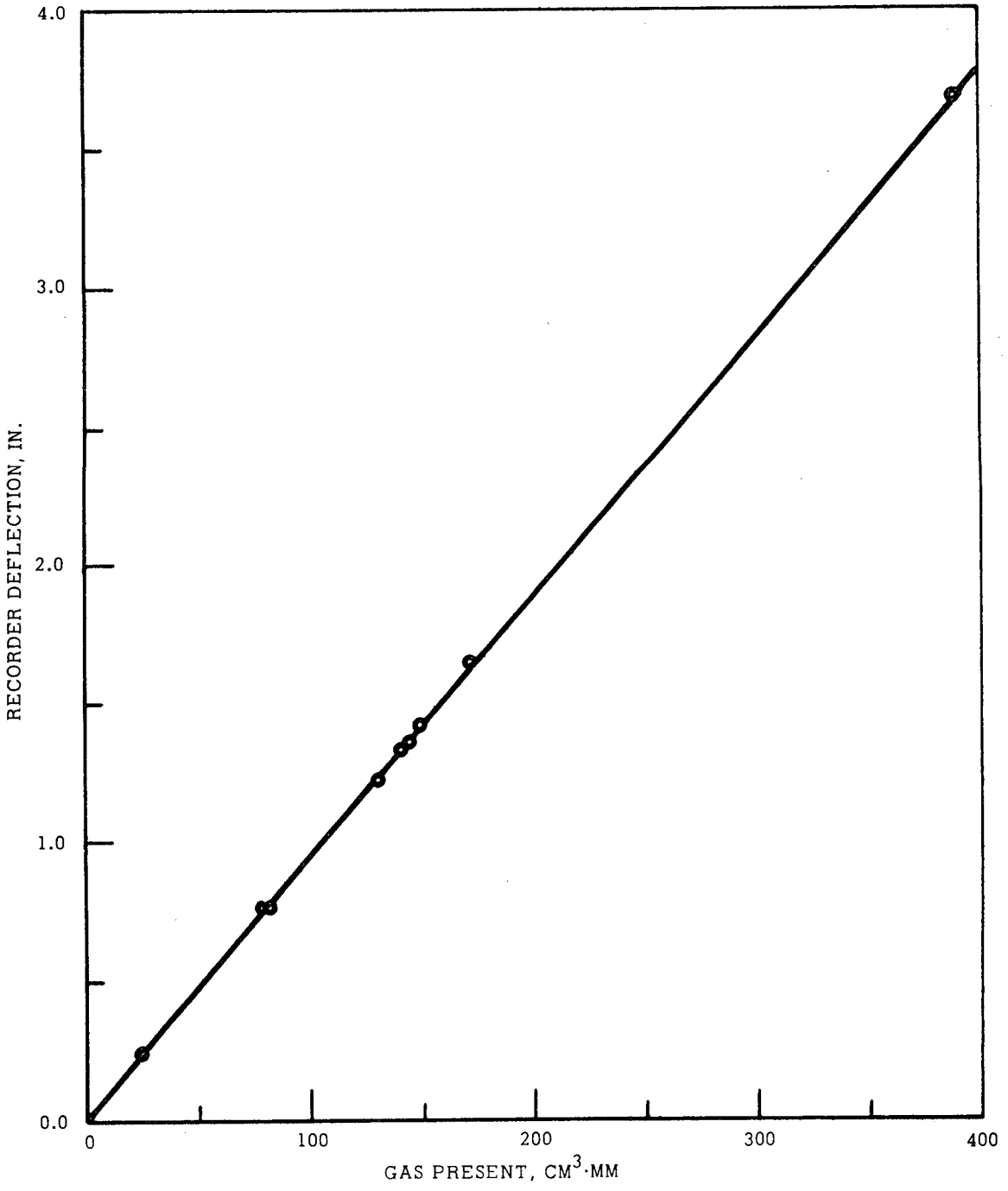

Fig. 3. Recorder Response After 20-Fold Amplification of Gage Output with Respect to the Quantity of Gas Present as Measured at Room Temperature.

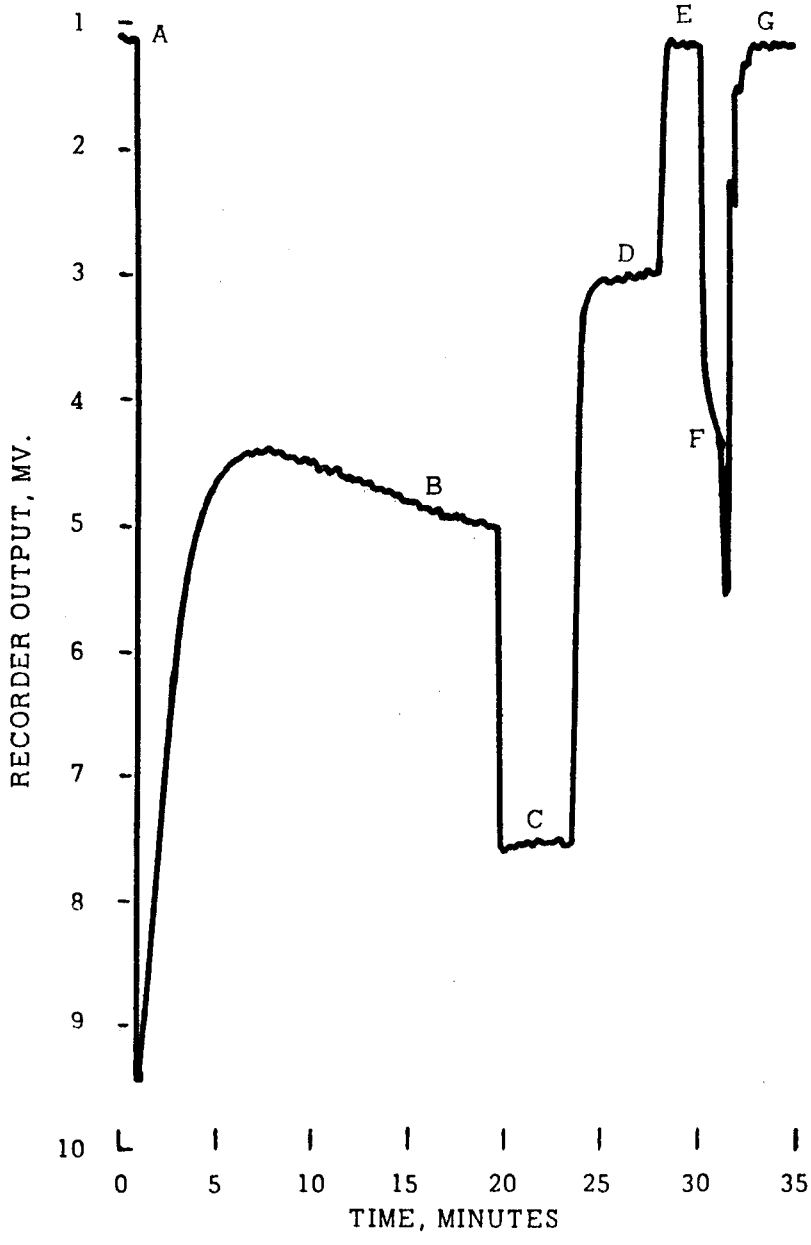

Fig. 4. Pressure-Time Recording during a Vacuum-Fusion Oxygen Determination. A, sample introduction; B, blank rate; C, dynamic circulation pressure; D, CO_2 removed by freezing; E, non-condensable gases exhausted; F, CO_2 released; G, CO_2 transferred by Toepler pump to McLeod gage. (Gage output amplified 50 fold).

ADAPTATION OF THE CEC MODEL 21-611-1 MASS SPECTROMETER TO HYDROGEN ANALYSIS

by

D. E. Seizinger
L. A. Fergason
C. H. McBride

SUMMARY

The Consolidated Electrodynamics Corporation Model 21-611-1 mass spectrometer was adapted to the determination of hydrogen in uranium. The standard instrument was not completely suitable for the hydrogen determination; therefore, several modifications were required to improve the over-all operation for this analysis.

INTRODUCTION

A previous report has described the mass spectrometric determination of hydrogen in uranium metal.[1] The adaptation of this method to an inexpensive mass spectrometer (Consolidated Electrodynamics Corporation Model 21-611-1) was desired in order to release the larger instrument for research and non-routine analysis. Modifications were made in the instrument and the method to increase the operating sensitivity, decrease the background, and reduce the noise level of the output.

EXPERIMENTAL

The sensitivity of the instrument was increased by shortening the standard capillary inlet leak from 12 inches to 3 inches. With the shorter capillary, more sample gas flowed into the instrument sample chamber, resulting in an increased pressure in this section. The higher pressure in the instrument sample chamber increased the sensitivity by a factor of 10.

Helium was used as the sweep gas to carry the outgassed hydrogen from the uranium metal past the mass spectrometer leak as described previously.[1] Investigation showed that the ionizing characteristics of this instrument produce doubly charged helium ions at m/e 2. Because of this characteristic, the background spectrum at m/e 2 was intolerably high. Consequently, purified argon was substituted for the helium, and a low m/e 2 background was obtained.

Vibrations created by the forepump mounted on the same console as the amplifier caused erratic electrical transients that were ascribed to a vibration-sensitive contact between the amplifier and the detector. Another result of this condition was a shifting base line. The vibration problem was eliminated by removing the forepump from the "Analyzer" console and placing the console on a sturdy table.

The instrument as modified has been running on a routine basis for five months requiring very little maintenance.

RESULTS

Comparison between vacuum extraction and mass spectrometric results was made on production dingot uranium metal containing hydrogen concentrations in the range of 2.0-7.6 ppm. The observed average difference was 0.03 ppm and was significant only at a 60% confidence level with the vacuum extraction results appearing high. This was based on 29 observations.

At lower concentrations of hydrogen (0.1-0.5 ppm), the observed average difference was 0.15 ppm and was significant at a 98% confidence level with vacuum extraction higher. This was based on eight observations.

Precision of the determination of hydrogen at the 95% confidence level was obtained from uranium metal whose hydrogen content was determined to be homogeneous. Results are shown in Table I.

Table I

Precision Study of Hydrogen Determination by the Mass Spectrometer

Level of Hydrogen ppm	Precision ppm	Number of Determinations
6.3	±0.24	10
3.3	±0.07	18

ACKNOWLEDGMENT

The authors wish to express their appreciation to Mr. R. T. Springgate for the statistical treatment of the data, Mr. J. T. Renshaw for the vacuum extraction analyses and Mr. J. F. Frappier for the mass spectrometric analyses.

Reference

[1] L. A. Fergason, D. E. Seizinger, and C. H. McBride, Nuclear Sci. and Eng. 10 (No. 1), 53-6 (1961).

Glossary of Specialized Terms

billet - a bar of uranium suitable for subsequent rolling or extrusion

black oxide - U_3O_8

brown oxide - UO_2

core - rods of uranium machined to specific diameter and lengths. Cores, when canned, are used as fuel elements.

derby - the uranium metal product of the nominal 300-, 100-, and 50-lb reduction bombs that is subsequently recast

dingot - (direct ingot) the uranium metal product of 1400- and 3300-lb reduction bombs. This metal not recast.

green salt - UF_4 containing small amounts of UO_2F_2 and uranium oxides

ingot - recast uranium metal

MFL - magnesium fluoride liner

orange oxide - UO_3

rod - cylindrical length of uranium produced by rolling or extruding uranium billets and ingots

tube - cylindrical length of uranium produced by extruding hollow uranium billets and ingots

UNH - uranyl nitrate hexahydrate